JOURNAL OF GEOPHYSICAL RESEARCH, VOL. 100, NO. B1, PAGES 475–496, JANUARY 10, 1995

Experiments on flow focusing in soluble porous media, with applications to melt extraction from the mantle

Peter B. Kelemen,[1] J. A. Whitehead,[2] Einat Aharonov,[3] and Kelsey A. Jordahl[4]
Woods Hole Oceanographic Institution, Woods Hole, Massachusetts

Abstract. We demonstrate finite structures formed as a consequence of the "reactive infiltration instability" (Chadam et al., 1986) in a series of laboratory and numerical experiments with growth of solution channels parallel to the fluid flow direction. Regions with initially high porosity have high ratios of fluid volume to soluble solid surface area and exhibit more rapid fluid flow at constant pressure, so that dissolution reactions in these regions produce a relatively rapid increase in porosity. As channels grow, large ones entrain flow laterally inward and extend rapidly. As a result, small channels are starved and disappear. The growth of large channels is an exponential function of time, as predicted by linear stability analysis for growth of infinitesimal perturbations in porosity. Our experiments demonstrate channel growth in the presence of an initial solution front and without an initial solution front where there is a gradient in the solubility of the solid matrix. In the gradient case, diffuse flow is unstable everywhere, channels can form and grow at any point, and channels may extend over the length scale of the gradient. As a consequence of the gradient results, we suggest that the reactive infiltration instability is important in the Earth's mantle, where partial melts in the mantle ascend adiabatically. Mantle peridotite becomes increasingly soluble as the melts decompress. Dissolution reactions between melts and peridotite will produce an increase in liquid mass and lead to formation of porous channels composed of dunite (> 95% olivine). Replacive dunite is commonly observed in the mantle section of ophiolites. Focused flow of polybaric partial melts of ascending peridotite within dunite channels may explain the observed chemical disequilibrium between shallow, oceanic mantle peridotites and mid-oceanic ridge basalts (MORB). This hypothesis represents an important alternative to MORB extraction in fractures, since fractures may not form in weak, viscously deforming asthenospheric mantle. We also briefly consider the effects of crystallization, rather than dissolution reactions, on the morphology of porous flow via a second set of experiments where fluid becomes supersaturated in a solid phase. Formation of short-lived conduits parallel to the flow direction occurs rapidly, and then each conduit is eventually choked by interior crystallization; fluid flow then passes through the most permeable portion of the walls to form a new conduit. On long time scales and length scales, transient formation and destruction of conduits will result in random and diffuse flow. Where liquid cools as it rises through mantle tectosphere on a conductive geotherm, it will become saturated in pyroxene as well as olivine and decrease in mass. This process may produce a series of walled conduits, as in our experiments. Development of a low-porosity cap overlying high porosity conduits may create hydrostatic overpressure sufficient to cause fracture and magma transport to the surface in dikes.

Introduction

This paper reports initial results of an experimental and numerical study of focused flow of fluids through dissolution channels in partially soluble porous media. These results are relevant to understanding melt extraction from the Earth's upper mantle. Strongly focused flow, which limits solid/liquid interaction during melt extraction, is required to explain the localization of magmatism at mid-ocean ridges and the composition of mid-ocean ridge basalts and residual peridotites. By contrast, more diffuse flow of liquids combined with substantial mantle/magma interaction may be indicated by the geochemistry of subduction-related magmas, within-plate volcanics, and samples of the mantle tectosphere. Results of this study will also have relevance to a variety of other work in the Earth sciences and related fields. For example, they may help to explain the nature of hydrothermal vents along mid-ocean ridges, where strongly focused discharge of cooling fluid seems to characterize fluid circulation.

The simplest experiments presented here involve flow of water through a mixture of glass balls and salt (NaCl) grains combined into an approximately homogeneous mixture within a narrow, rectangular glass chamber. Water is introduced at the open top of

[1]Department of Geology and Geophysics, Woods Hole Oceanographic Institution, Woods Hole, Massachusetts.
[2]Department of Physical Oceanography, Woods Hole Oceanographic Institution, Woods Hole, Massachusetts.
[3]WHOI/MIT Joint Graduate Program in Oceanography, Department of Earth, Atmospheric, and Planetary Sciences, Massachusetts Institute of Technology, Cambridge, Massachusetts.
[4]WHOI/MIT Joint Graduate Program in Oceanography, Woods Hole Oceanographic Institution, Woods Hole, Massachusetts.

Paper number 94JB02544.
0148-0227/95/94JB-02544$05.00

this chamber, then flows down through the matrix of glass balls and salt, through a layer of foam, and finally exits through small outlet holes at the base. The initial interface or "front" between salt-free and salt-bearing glass balls is planar and horizontal, perpendicular to the flow direction of the water flowing down through the tank. However, within minutes, this front becomes unstable, resulting in focused porous flow of water within elongate, salt-free dissolution channels parallel to the flow direction. Our numerical computer simulations of these experiments show the same qualitative behavior. Chadam and others [*Chadam et al.*, 1986; *Ortoleva et al.*, 1987] have suggested a simple mechanism for this instability, which they termed the "reactive infiltration instability": small perturbations in porosity are amplified due to two positive feedback mechanisms: (1) in a high-porosity region, a higher water volume to solid surface area ratio leads to lower instantaneous salinity and more rapid dissolution of salt, and (2) higher-porosity regions permit more rapid ingress of water that is not saturated in salt, leading to additional dissolution of salt. For both these reasons, initial perturbations in porosity cause formation of dissolution channels parallel to the flow direction.

Many workers have observed features in the upper mantle section of ophiolites which were formed by melt/rock reaction during focused porous flow of ascending liquid through peridotite. The most striking of these are dunites, rocks composed almost entirely of the mineral olivine. Some dunites in the upper mantle form by replacement of surrounding peridotite, as melt migrating by intergranular flow dissolves pyroxene minerals from the porous matrix through which it passes (Figure 1). Melt flow may be focused during formation of replacive dunites because dunite is more permeable than surrounding peridotite, in a process analogous to the focusing of flow in our experiments. Formation of dunite "conduits" during reaction between olivine-saturated liquid and harzburgite has been experimentally demonstrated on a centimeter scale by *Daines and Kohlstedt* [1993].

The melt/rock reaction process which initially forms dunite from peridotite may have profound effects on the composition of derivative liquids [e.g., *Kelemen*, 1990]. However, once a dunite channel is formed, focused flow through the channel may leave successive liquids virtually unchanged. Formation of melt conduits as a result of chemical dissolution represents an important alternative to melt extraction by flow through cracks and thus may be particularly important in explaining extraction of mid-ocean ridge basalt from the viscously deforming asthenosphere. Even where transport through melt-filled cracks is the dominant mode of melt extraction from the mantle, formation of porous conduits may be important in creating hydrostatic pressure sufficient to cause fracture.

This paper is divided into four parts. The introduction describes current problems in understanding melt extraction from the mantle, with an emphasis on mid-ocean ridges, summarizes evidence for porous flow of melt through peridotite in the upper mantle, and summarizes some prior work on focusing of fluid flow in partially soluble porous media. In the second section, the results of experiments on water flowing through salt are used to elucidate the dynamic instability of diffuse porous flow in a soluble matrix. In the third section, the results of numerical experiments are discussed. These confirm and quantify some observations from the laboratory experiments and extend them to systems in which there is a gradient in solubility of the solid matrix, rather than a sharp initial solution front. In the final section, these results are related to the structure of porous flow of melt in the mantle, and the potential geochemical effects of flow focusing in different magmatic-tectonic environments are discussed.

Melt Extraction From the Mantle at Mid-Ocean Ridges

Recent geochemical investigations suggest that in some tectonic settings and on some length scales, porous flow of melt in the mantle is the dominant mode of melt extraction. The evidence for porous flow includes field observations of replacive dunites [e.g., *Boudier and Nicolas*, 1977; *Dick*, 1977; *Quick*, 1981; *Kelemen*, 1990; *Kelemen et al.*, 1992], experimental results [e.g., *Watson*, 1982; *Riley and Kohlstedt*, 1991], and theoretical investigations [e.g., *Maaloe and Scheie*, 1982; *McKenzie*, 1984]. Experiments have repeatedly demonstrated porous flow of melt in mantle lithologies can occur at rates of tens to hundreds of centimeters per year, whereas plate velocities (half spreading rate) are of the order of 1-10 cm yr^{-1}.

Extremely depleted abyssal peridotites, dredged from fracture zones along the mid-ocean ridges, are the residues of partial melting which formed mid-ocean ridge basalts (MORB), but they are far from trace element equilibrium with aggregate MORB liquids [*Johnson et al.*, 1990; *Johnson and Dick*, 1992]. This has been ascribed to a fractional or incremental melting process, in which the aggregate liquid produced is MORB, while the solid residue records equilibrium with the last, most depleted melt fraction to be extracted. Since this aggregate liquid is extracted from the source in very small increments (less than one volume percent of the rock), it must initially move by porous flow. Similar explanations have been advanced for large fractionations of the Sm/Nd and Lu/Hf ratios between source and liquid which occur during extraction of MORB from the mantle [*Salters and Hart*, 1989]. This chemical evidence confirms theoretical suggestions that melt mobility due to porous flow permits efficient extraction of small increments of partial melt from mantle peridotite and therefore favors a near-fractional melting process [e.g., *McKenzie*, 1984].

Acceptance of the growing body of evidence for porous flow as an important mechanism for melt transport in the shallow mantle raises a number of fundamental problems for geochemists and geophysicists studying partial melting in the mantle and accretion of the oceanic crust. These problems are summarized below:

1. The composition of abyssal peridotite presents a seeming paradox: Large fractionations of incompatible trace elements in abyssal peridotites require the continual removal of small melt increments by porous flow. Yet, if porous flow is the dominant mechanism of melt transport beneath the mid-ocean ridges, then why are the shallowest mantle samples unaffected by interaction with liquids derived from deeper in the column of decompressing mantle? Small degree melts, derived from partial melting of garnet peridotite at pressures exceeding about 2.5 GPa, are the first increments of melting during decompression of mantle beneath mid-ocean ridges [e.g., *Salters and Hart*, 1989]. Such liquids are enriched in light rare earth elements and other incompatible elements. If these melts traversed the overlying column of mantle by uniformly distributed porous flow, chemical interaction would return light rare earth and other incompatible trace elements to the peridotite, so that shallow mantle peridotites would have higher concentrations of these elements than are observed in abyssal peridotite.

Spiegelman and Kenyon [1992] attempted to resolve this paradox by suggesting that melt segregates into "veins" or channels

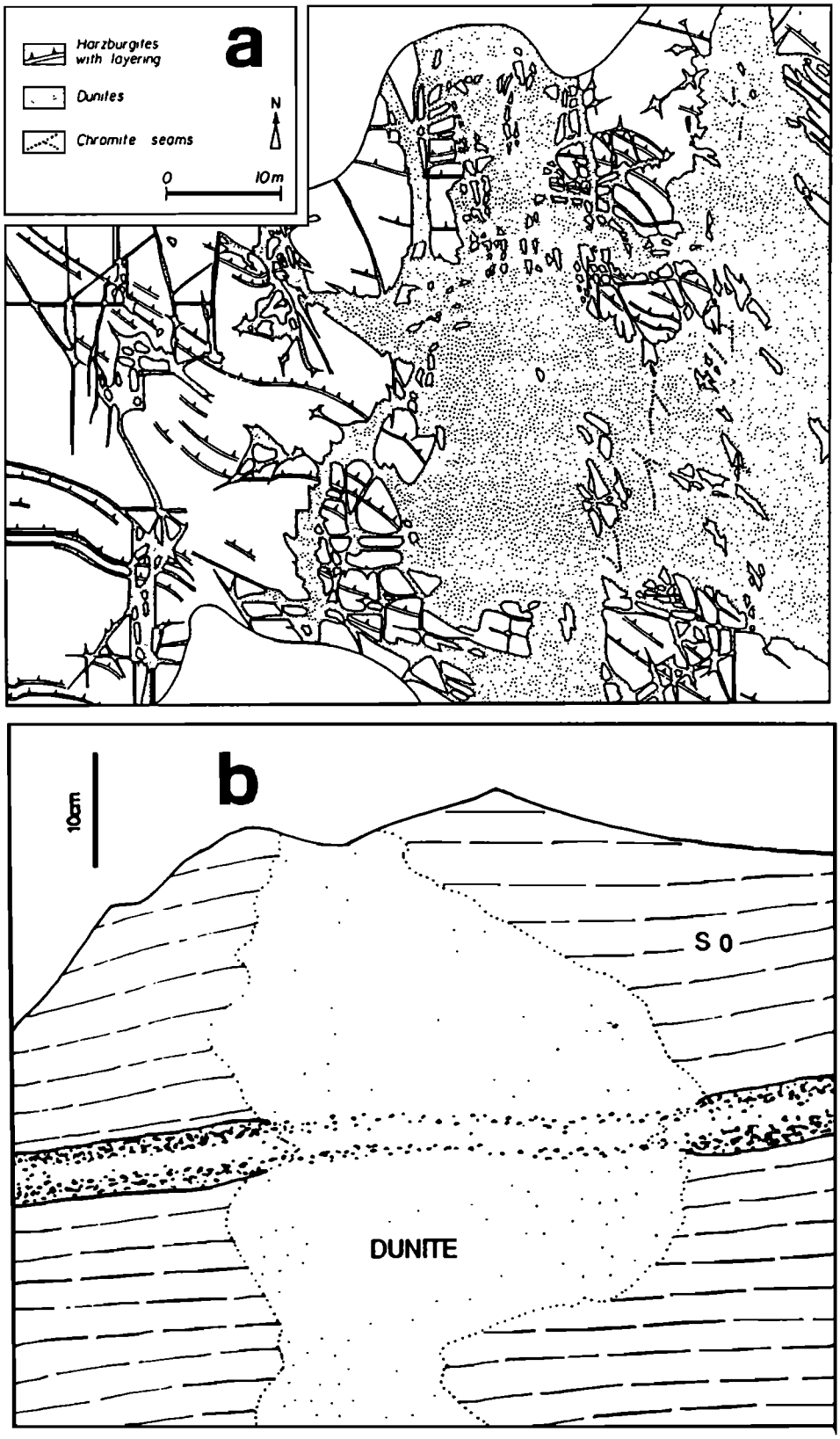

Figure 1. (a) Outcrop map of discordant dunite cutting mantle peridotite in an ophiolite in the polar Urals, from *Nicolas* [1989], after *Savel'yeva et al.* [1980]. Several aspects of the contact relationships between dunite and peridotite indicate that the dunites were formed by near constant volume replacement of peridotite, as a result of dissolution of pyroxene, combined with crystallization of olivine, in a liquid migrating by porous flow through the mantle. Anastamosing dunite encloses islands of relict peridotite whose outlines would not match the adjacent walls if dunite were removed. Pyroxenite layers in the peridotite are locally, selectively replaced by narrow dunites. Pyroxenite layers in the peridotite are not offset but instead have been replaced, where they intersect dunite at an angle. (b) Sketch of an outcrop in the Lanzo peridotite, from *Nicolas* [1989], after *Boudier and Nicolas* [1977], showing dunite replacing peridotite with a pyroxenite band. Replacement of the relatively chrome rich pyroxenite by dunite formed a train of relict, chromian spinel in the dunite, indicating that the dunite formed by in situ replacement rather than as an intrusive dike later filled by olivine crystals. Both (a) and (b) reprinted by permission of Kluwer Academic Publishers.

spaced at least 10 cm apart. Following segregation, they no longer interact chemically with their solid matrix. Similarly, *Hart* [1993] suggested that melt extraction occurs along a network of coalescing tubes with a fractal structure. Melt moves rapidly through large tubes and is out of equilibrium with surrounding mantle peridotite after the melt has moved more than 1 km from its source region. Nicolas and co-workers [e.g., *Nicolas*, 1990] propose that development of an interconnected porous melt network, over a 10-km depth interval, leads to magmatic overpressure, followed by hydrofracture and rapid melt extraction along cracks. A weakness of the cracking hypothesis is that partially molten, low-viscosity asthenosphere may not be strong enough to support sufficient stress to induce fractures. In the present study we hope to elucidate the mechanisms which can form melt veins or channels, the conditions under which they form, and the length scales and aspect ratios of the resulting conduits. Formation of dissolution channels, perhaps ultimately producing small open conduits, may represent a viable alternative to the cracking hypothesis.

2. Geophysical models of melting and crustal accretion at mid-ocean ridges also involve a paradox: In order to produce observed crustal compositions and volumes, upwelling mantle must pass through its solidus over a broad zone beneath spreading centers, much wider than the zone of active crustal accretion at the ridges. Why, then, is the active volcanic and plutonic zone so narrow? Some models propose focused asthenospheric flow (much faster than plate velocities) directly beneath ridges [e.g., *Rabinowicz et al.*, 1984, 1987; *Scott and Stevenson*, 1989]. Other solutions involve two-phase flow in the partially molten upper mantle: Melt flow converges toward the ridge, while the solid matrix diverges from the ridge to form part of the lithosphere [e.g., *Spiegelman and McKenzie*, 1987]. Some hypotheses presume that porous channels form in the mantle. For instance, *Spiegelman* [1993] suggested that decreasing melt porosity near the asthenosphere/"lithosphere" boundary (as defined by the mantle peridotite solidus) produces planes of focused melt flow in the asthenosphere, parallel to the base of the lithosphere. The present study may advance understanding of this process.

In this paper, it is suggested that melt extraction from the shallow mantle beneath mid-ocean ridges is focused in narrow conduits by the inherent instability of diffuse flow through partially soluble porous media. Additionally, under certain circumstances, conduits for focused flow may develop hydrostatic overpressure sufficient to form melt filled cracks at their tops, as proposed by Nicolas and co-workers [e.g., *Nicolas*, 1990], or melt-filled pockets as proposed by *Sleep* [1988, Produc-

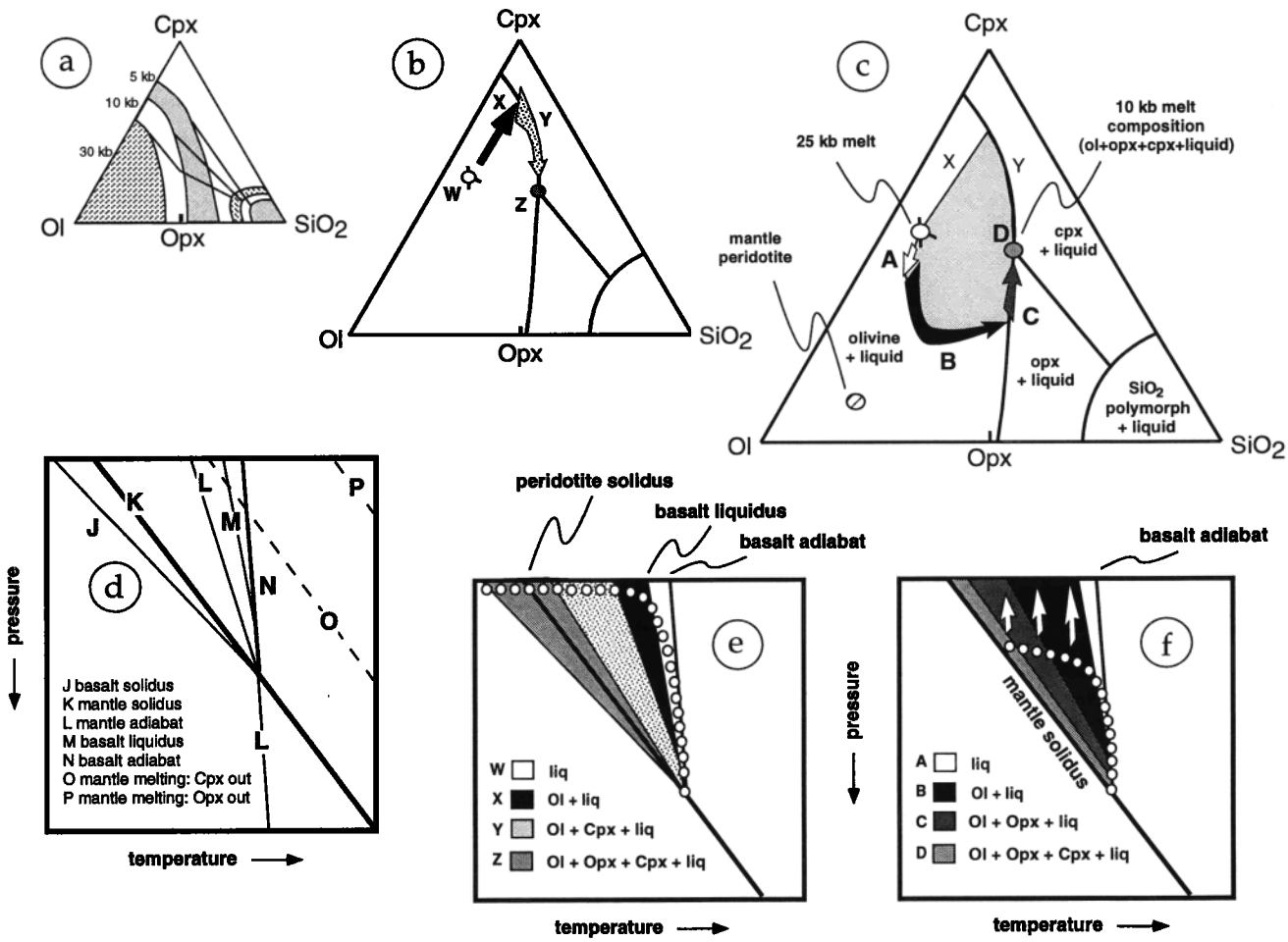

Figure 2. Liquid and solid products of reaction between ascending melts and surrounding upper mantle wall rocks are illustrated in these diagrams. At the top are three schematic, pseudo-ternary phase diagrams on the plane olivine (Ol) - clinopyroxene (Cpx) - silica (SiO_2), projected from spinel, for hydrous silicate liquids at upper mantle pressures [*Kelemen et al.*, 1992]. (a) The effect of pressure in this system. Decreasing pressure leads to increased stability of Ol relative to pyroxenes, so that liquids in equilibrium with Ol, Cpx, and Opx at a

tion of veins by magma solitons, submitted to *Journal of Geophysical Research*, 1994]. Focused flow of melt in coalescing conduits and cracks beneath mid-ocean ridges, perhaps converging beneath the center of individual ridge segments, would leave much of the shallow mantle unaffected by chemical exchange with liquids from deeper in the melting column. High melt/rock ratios in these conduits would produce highly porous dunites, equilibrated with ascending melt, so that ascending liquids may remain out of equilibrium with mantle peridotite surrounding the conduits. Mixing in focused flow zones would produce a relatively uniform liquid composition in the mantle, which would then be delivered as aggregate MORB during crustal accretion.

Evidence for Focused Melt Flow in the Upper Mantle: Formation of Replacive Dunites

Field studies have demonstrated that focused porous flow of melt has occurred in the upper mantle. The most obvious features formed by focused melt flow are bodies of dunite (composed of >95% olivine). These occur in a variety of morphologies, ranging from large, generally elongate, lensoid bodies, often including concentrations of "cumulate" chromite, through smaller, commonly tabular bodies which can often be shown to be replacive of surrounding, pyroxene-bearing peridotite [e.g., *Boudier and Nicolas*, 1977; *Dick*, 1977; *Quick*, 1981; *Kelemen*, 1990; *Kelemen et al.*, 1992], to small, irregular patches. Some dunites have been considered to be cumulate dikes, i.e., products of crystal fractionation filling cracks, which were initially filled with olivine-saturated melt. While this process may have formed some dunite bodies in their entirety and may contribute to the formation of many others, this discussion will concentrate upon those dunite bodies which have demonstrably formed by replacement processes during porous flow of melt. These replacive bodies of dunite form by dissolution of pyroxene, combined with precipitation of olivine, in decompressing melts infiltrating along grain boundaries. Such dunites have been shown to be replacive on the basis of their contact relationships (Figure 1).

While mantle dunites are best known in the mantle sections of ophiolites, within the upper 15 km of the mantle beneath thin, oceanic crust, they are also found in peridotites of deeper provenance. For example, there are garnet-bearing dunite xenoliths derived from depths exceeding 90 km in Hawaii [*Sen and Jones*, 1990] and Siberia [*Sobolev et al.*, 1973; *Pokhilenko et al.*, 1977]. Dunites derived from more than 30-40 km depth are abundant in

high pressure will be saturated only in Ol during cooling at a lower pressure. (b) The effect of decompression from 2 to 0.5 GPa, cooling, and closed-system, crystal fractionation upon a picritic (high Mg basalt) liquid formed by a small degree of partial melting of mantle lherzolite at 2 GPa. The adiabatically ascending liquid at point W is initially undersaturated in solids. As it cools and diverges from an adiabatic PT path, it saturates first in Ol. Fractionation of Ol drives the liquid to saturation in Cpx along the vector labeled X, after which coprecipitation of Ol + Cpx, and reaction between liquid and Ol producing Cpx, drives the liquid along the vector labeled Y. Finally, saturation in Opx is reached at point Z. The liquid composition at Z will be substantially different from a partial melt of lherzolite at 0.5 GPa, having a lower Mg/Fe ratio and lower Ni and Cr contents than a mantle melt. (c) Reaction at 2 to 0.5 GPa between mantle lherzolite and the same picritic liquid as in Figure 2b. The peridotite reactant is just at its solidus temperature at 0.5 GPa. Liquid rising adiabatically is above its liquidus temperature. For this reason, along path A, the melt initially dissolves peridotite. This leads to olivine saturation in the liquid, which will crystallize Ol, and continue to dissolve pyroxene. One possible liquid path is shown as the vector labeled B; this is for relatively rapid reaction and slow cooling, during which liquid mass increases. More rapid cooling, or slower pyroxene dissolution, would produce derivative liquid compositions within the shaded region bounded by B, C, X, and Y. Eventually, path B leads to saturation of the melt in Opx as well as Ol. Continued reaction and cooling will consume Cpx and a small amount of Ol from peridotite reactants, producing decreasing liquid mass, Opx + Ol solid assemblages, and derivative liquids along path C. Finally, at D, the liquid will become saturated in Cpx. The liquid composition at point D will be similar in major element composition(Mg/Fe, Ni, Cr, SiO_2) to a small degree melt of mantle lherzolite at 0.5 GPa, although its trace element characteristics may preserve a "memory" of its open system provenance. At bottom are PT plots summarizing the composition of liquid and solid products of the polybaric crystallization and reaction processes illustrated above. (d) General features of adiabatic ascent paths for solids and liquids in the mantle, relative to the slope of the mantle solidus and the saturation surface for olivine in mantle-derived liquids [e.g., *Yoder*, 1976; *McKenzie and Bickle*, 1988]. If liquid ascends to the surface along an adiabatic PT path in a closed system, it will remain undersaturated in solids, retaining the composition of a partial melt of mantle peridotite at high pressure. If it ascends in an open system, it will be capable of dissolving solid phases from surrounding peridotite, resulting in a net increase in liquid mass. Where it cools to temperatures lower than along the adiabatic ascent path, it will saturate first in Ol. Adiabatically ascending mantle peridotite follows a less steep PT path, due to the energy requirements of fusion during ascent. The lherzolite solidus has a much shallower PT slope than adiabatic ascent paths. Ascending mantle lherzolite will gradually generate partial melt, consuming pyroxene as it does so. Cpx is generally not completely consumed by closed system partial melting during adiabatic ascent beneath mid-ocean ridges [e.g., *Dick et al.*, 1984]. By contrast, reaction with ascending liquid can completely dissolve all pyroxene from lherzolite. (e) Products of the polybaric, closed system crystal fractionation path illustrated in Figure 2b. Liquid mass remains constant over the adiabatic portion of the ascent path, then decreases during conductive cooling. (f) Products of the polybaric reaction process illustrated in Figure 2c. Liquid mass increases during the initial portion of the ascent path in which the liquid is under-saturated in solids and also over part of the path in which the liquid is saturated only in olivine. As the liquid continues to cool, liquid mass begins to decrease, and the liquid becomes saturated in pyroxene as well as olivine.

continental xenolith suites [e.g., *Nixon*, 1987]. Replacive dunites are found within the Ronda peridotite massif [*Remaidi*, 1993; *Garrido et al.*, 1993], interpreted to have formed at depths from 40 to 15 km. Replacive dunite bodies, replacing pyroxene-rich peridotites and pyroxenites, are also observed in crustal rocks, within the ultramafic portions of many large, mafic layered intrusions, including the Bushveld intrusion in South Africa [e.g., *Stumpfl and Rucklidge*, 1982], the Stillwater intrusion in Montana [e.g., *Raedeke and McCallum*, 1984], and the Rhum intrusion in Scotland [e.g., *Butcher et al.*, 1985], as well as in smaller, zoned ultramafic-felsic intrusions [e.g., *Aho*, 1956; *James*, 1971; *Irvine*, 1974; *Kelemen and Ghiorso*, 1986].

Mass and Energy Balance in Formation of Replacive Dunites

As noted by *Sleep* [1975], ascending partial melts of mantle peridotite, if they rise adiabatically, will be above their liquidus temperature at pressures lower than the pressure of melting (Figure 2). If they are in contact with solid phases in the overlying mantle, these melts will dissolve solids until the combined effects of conductive cooling, cooling due to the endothermic effect of dissolution reactions, and compositional change due to dissolution reactions return them to saturation in olivine. *Sleep* [1975, also personal communication, 1994] calculated that average basaltic melts ascending beneath spreading centers might dissolve several percent of their mass due to this thermal effect alone. Subsequent to olivine saturation, pyroxene dissolution combined with precipitation of a smaller mass of olivine will continue to increase the liquid mass and the porosity in the solid matrix. These reactions were analyzed thermodynamically by *Kelemen* [1990], who found that the exothermic effect of olivine crystallization nearly balances the endothermic effect of pyroxene dissolution. Kelemen noted that the apparent heat of crystallization of olivine, per gram, at typical magmatic temperatures is about 1.3 times larger than the apparent heat of fusion of pyroxenes, so that reactions at constant pressure between olivine-saturated liquid and pyroxene-bearing solids increase the mass of liquid under conditions of constant enthalpy or constant temperature. This prediction has been confirmed experimentally by *Daines and Kohlstedt* [1993]. Where pressure decreases, as for ascending solids and liquids beneath a mid-ocean ridge, liquid mass will increase still more.

As can be seen in the phase diagrams of Figure 2, the total solubility of pyroxene in olivine-saturated, mantle-derived magmas is dependent upon their composition and upon the temperature and pressure of the dissolution reaction. A simple rule is that the larger the difference between the pressure of initial melting and the final pressure of reaction, the larger the solubility of pyroxene in a given liquid [e.g., *Stolper*, 1980]. Other variables, such as the changing alkali and H_2O content of the liquid as it reacts, play an important role in determining the solubility. For this reason, it is impossible to use two- and three-dimensional phase diagrams for accurate estimation of pyroxene solubility in natural, multi-component magmas. *Kelemen* [1990] used a thermodynamic solution model for silicate liquids [e.g., *Ghiorso et al.*, 1983; *Ghiorso*, 1985; *Ghiorso and Kelemen*, 1987] to calculate melt-rock reaction effects in natural systems. These calculations were limited, in part, due to the difficulty of accurately calculating melt compositions at low melt fractions. A new version of the model [*Ghiorso and Sack*, 1993, 1994] is now available. This new version incorporates minor components, such as sodium and titanium, in solid phases such as pyroxenes and oxides and therefore can predict the equilibrium mode and composition of systems including small melt fractions.

We used this new version of the solution model to calculate the solubility of mantle peridotite in basaltic liquids beneath a mid-ocean ridge. The results are illustrated in Figure 3. Calculations were made for a pressure of 0.2 GPa, using two liquid compositions (Table 1): (1) a picritic liquid produced at small degrees of melting of mantle lherzolite at about 2 GPa and 1350°C, and (2) a tholeiitic liquid with a magnesian mid-ocean ridge composition, produced by 12% melting of mantle lherzolite at 1 GPa and 1325°C, close to the conditions inferred for average mid-ocean ridge basalt [e.g., *Kinzler and Grove*, 1992; *Langmuir et al.*, 1992]. The solid reactant was a depleted peridotite composition typical of abyssal peridotites dredged from the mid-ocean ridges [e.g., *Dick*, 1989].

These calculations incorporate the effect of temperature as well as pressure. If partial melts beneath "normal" mid-ocean ridge segments (potential temperature $\leq$ 1400°C) rose in a chemically closed system, they would have temperatures ranging from more than 1350°C to about 1200°C, depending upon the pressure of melting [e.g., *McKenzie and Bickle*, 1988], with an average close to 1275°C. The solid material rising beneath a ridge undergoes partial melting and therefore is cooled by the endothermic effect of the enthalpy of fusion. It may reach the top of the adiabatic upwelling regime, near the base of the crust, at temperatures ranging from about 1275° to 1200°C. At any given pressure, adiabatically ascending liquids in a closed system would be hotter (up to 100°C hotter) than adiabatically ascending peridotite undergoing partial melting. Thus melt/rock reaction involves a combination of processes: solution of solid phases into superliquidus magma, dissolution of pyroxene in olivine-saturated magma, and conductive cooling of hot liquid passing through cooler solids. A typical pressure-temperature path for a high-pressure melt might begin at 1350°C and 2 GPa, and end at 1300°C and 0.2 GPa, near the base of the crust. An average mid-ocean ridge melt interacting with ascending peridotite might begin at 1325°C and 1 GPa and end at 1275°C and 0.2 GPa. As can be seen in Figure 3, the solubility of peridotite under these conditions is found to be about 25% in the high-pressure, picritic melt, and 3-15% in the magnesian mid-ocean ridge basalt. By contrast, the solubility of olivine in these liquids in the temperature range of interest is small, so that reaction with dunite during ascent has a comparatively minor effect on the mass of ascending liquids.

The phase proportions of the reaction products at 1300° and 1275°C are also illustrated in Figure 3. The high-pressure, picritic melt dissolves enough pyroxene to convert 4 times its mass in harzburgite to pyroxene-free dunite. The lower-pressure, magnesian mid-ocean ridge basalt melt converts one equivalent mass of harzburgite to dunite. From these calculations, we may conclude that ascending melts beneath mid-ocean ridges are capable of producing substantial additional porosity by dissolution reactions and can leave behind a mass of dunite in the upper mantle equivalent to the mass of the oceanic crust. These calculations are for the maximum extent of reaction, since they presume that all ascending melt reacts with mantle harzburgite. If kinetic factors inhibit reaction, or if melt flow is focused into nonreactive dunite channels, then less porosity will be created by reaction and less dunite will be formed.

These calculations of the mass of dunite which can be produced by reaction may be compared with observed proportions of dunite in the upper mantle section of ophiolites. *Lippard et al.* [1986] summarized estimates of the proportion of dunite in the Oman ophiolite. A variety of French, British, and American workers have estimated that dunite comprises from 5 to 15% of

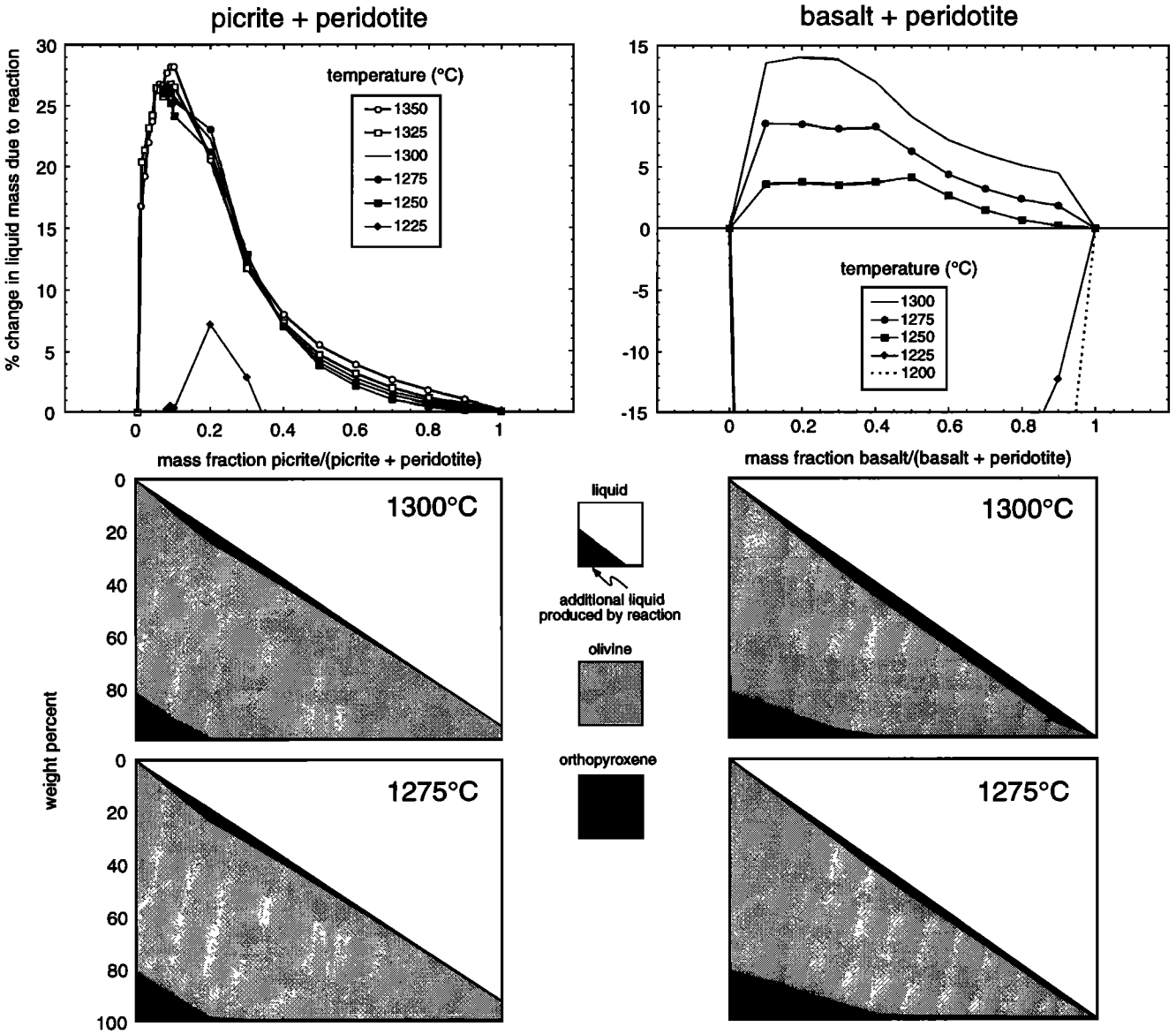

Figure 3. Results of thermodynamic modeling of reaction between liquids and mantle peridotite at 0.2 GPa, on the quartz-magnetite-fayalite oxygen buffer, using a solution model for natural silicate liquids and coexisting minerals [*Ghiorso and Sack*, 1993, 1994]. Solid and liquid compositions used in modeling are given in Table 1. Input required for the model is pressure, temperature, oxygen fugacity, and bulk composition. Output includes the proportions and compositions of solid and liquid phases predicted to be present at equilibrium. Results are presented in two columns, the left-hand one for picritic magma plus peridotite, and the right-hand one for basaltic magma plus peridotite. The x axis in all diagrams is the mass fraction of the magmatic component, varying from pure peridotite (0, on left) to pure picrite or basalt (1, on right). The top two diagrams illustrate the percent change in liquid mass due to isothermal reaction, as a function of the mass fraction of the magmatic component. This value is calculated as 100% (1 - mliq/mliq'), where mliq is the mass of liquid calculated by the model to be present in a given bulk composition at 0.2 GPa and a specified temperature, and mliq' is the mass of liquid which would be present in a linear combination of the peridotite and magma compositions at the same temperature and pressure. The bottom four diagrams illustrate the equilibrium proportions of solid and liquid phases present as a function of the mass fraction of the magmatic component. A small amount (<2%) of Cr-Al spinel is present in all bulk compositions except the pure picrite end-member but has been omitted for clarity.

the 10 to 15 km thick mantle section. If the dunites represent channels of focused melt flow, this suggests that most upwelling of melt is confined to about 10% of the total volume of the shallow mantle. The mass balance calculations in this section suggest that the maximum amount of dunite which could form would be equivalent to the amount of melt formed beneath the ridge, equivalent to the average percentage of partial melting (about 10% [e.g., *Kinzler and Grove*, 1992; *Langmuir et al.*, 1992]) . However, the proportion of dunite probably increases from near zero near the bottom of the melting column to a maxi-

Table 1. Compositions of Magmatic Components and Peridotite Used in Modeling

	Depleted Oceanic Peridotite[a]	5% melt of depleted lherzolite at 2 GPa[b]	12% melt of depleted lherzolite at 1 GPa[c]
SiO_2	42.97	47.5	50.49
TiO_2	0.00	1.0	0.65
Al_2O_3	0.79	17.7	17.94
Cr_2O_3	0.25	0	0.11
all Fe as FeO	8.27	8.5	6.69
MgO	45.83	12.0	10.08
CaO	0.76	8.0	11.37
Na_2O	0.01	5.0	2.47
K_2O	0.00	0.3	0.09

Values in weight percent. For results, see figure 3 and text.

[a]Average composition of abyssal peridotite dredged from the Bullard Fracture Zone, near the Bouvet Hot Spot, calculated from modal analysis combined with electron microprobe determination of phase compositions [*Dick*, 1989].

[b]Inferred composition of low degree melt of mantle lherzolite KLB-1 at 2.0 GPa, based on extrapolation from the experimental data of *Hirose and Kushiro* [1993].

[c]Experimentally determined composition of 12% melt of mantle lherzolite KLB-1 at 1.0 GPa [*Hirose and Kushiro*, 1993].

mal value near the base of the crust. Since all melt which forms the oceanic crust passes through the top few kilometers of upper mantle beneath a spreading ridge, the melt/rock ratio within this shallowest mantle must be much larger than 1:10, locally exceeding 1:1. In these regions, maximum possible dunite proportions could be quite large. However, once melt flow is focused in dunite conduits, then relatively little additional dunite will be formed by reaction. Thus observation of about 10% dunite in the shallow mantle section of ophiolites is well within the limits imposed by the mass balance calculations in this section.

Formation of dunite by reaction between decompressing melts and mantle peridotite may commonly increase the mass of liquid in the system and thus increase the total porosity. However, even where conductive cooling is important, so that melt mass remains constant or decreases slightly, formation of dunite from peridotite by melt/rock reaction will probably increase the effective permeability of the mantle. In laboratory experiments, an interconnected network of melt forms along olivine-olivine grain boundaries at liquid fractions less than 0.5 wt % [*Daines and Richter*, 1988], whereas pyroxene-olivine and pyroxene-pyroxene crystal intersections are rarely wetted by melt under H_2O-absent conditions, even with liquid fractions as high as 5 wt % [*Toramaru and Fujii*, 1986; *Von Bargen and Waff*, 1988; *Faul et al.*, 1993]. Thus we infer that dunite is more permeable than typical mantle lherzolite and harzburgite. Conversely, where conductive cooling and chemical effects of reaction lead to pyroxene saturation, products of melt/rock reaction will be pyroxene-rich, melt mass and porosity will decrease, and the permeability of regions traversed by migrating melt will be lower than in typical mantle lherzolite and harzburgite.

Morphology of Replacive Dunites

This section summarizes morphological features of replacive dunites in upper mantle peridotites for comparison with the results of laboratory experiments on formation of dissolution channels in soluble porous media. On a small scale, replacive dunites are very similar in all ophiolite mantle sections; they typically have sharp boundaries, with a transition from <2% pyroxene to >15% pyroxene over a few millimeters. This shows that reaction with migrating melt, rather than partial melting, was responsible for pyroxene-dissolution along the dunite margins. If these features were formed by in situ partial melting of mantle peridotite, then they would show a progressive, gradual depletion in pyroxene content. Gradational contacts could also be produced by melt/rock reaction, if dissolution rates were much slower than flow velocities, leading to substantial disequilibrium between migrating melt and mantle pyroxene on a local scale. Thus the typical presence of sharp contacts between dunite and peridotite suggests that local equilibrium was closely approached near these contacts. Liquid passing from dunite to peridotite became saturated in pyroxene over a few millimeters. Conversely, where liquid passed from peridotite to dunite, it became undersaturated in pyroxene over a few millimeters.

The most detailed maps of replacive dunites in mantle peridotite have been published for the Trinity peridotite by *Quick* [1981] and for an ophiolite in the Polar Urals by *Savel'yeva et al.* [1980]. Both sets of maps show a generally tabular structure for most dunites, particularly smaller ones. There is no single preferred orientation for the tabular dunites, and instead, the maps show an intersecting network of anastomosing channels. Both Quick and Savel'yeva et al. illustrate local, preferential replacement of preexisting, pyroxene-rich bands in the peridotite, which produces one trend in tabular dunite orientation. The presence of foliation, in the form of crystallographic preferred orientation or shape fabric in the original peridotite, may also result in anisotropic porosity and flow focusing. Thus some tabular, replacive dunites have probably inherited a relict tabular morphology.

Other tabular replacive dunites may reflect syntectonic focusing of porous flow in the presence of localized strain. *Kelemen and Dick* [1994] describe juxtaposition of ductile shear zones and syntectonically formed replacive dunites in the Josephine peridotite. Focused flow of melt and localized strain each provided positive feedback for the other. Specifically, deformation of crystals near the brittle/ductile transition probably created excess porosity and reduced pressure between plastically deforming grains. In addition, once deformation created an anisotropic shape fabric and/or crystallographic fabric in the peridotite, this may have enhanced the permeability in flow directions parallel to the shear zones [e.g., *Waff and Faul*, 1992]. At the same time, the presence of relatively high proportions of melt within regions of focused flow must have significantly lowered the bulk viscosity, which in turn further localized strain. Locally lower bulk viscosity in relatively melt-rich zones also may lead to locally lower effective pressure during deformation, thus increasing melt contents [*Stevenson*, 1989].

Observations of replacive dunite in mantle peridotite illustrate that porous flow is focused once the porosity structure is anisotropic, and thus many dissolution features inherit a tabular morphology imposed by deformation, or by other planar structures such as pyroxenite bands. By contrast, replacive dunites in crustal intrusions commonly form cylindrical "pipes," with irregular, anastomosing contacts against pyroxene-rich rocks. Such

pipelike features likely formed by focused flow of melt through solids which were initially isotropic in the horizontal dimension, under nearly hydrostatic stress. Cylindrical dissolution channels may be the natural result of the hydrodynamic channeling instability in the absence of planar anisotropy in the porous matrix. Sharp contacts between replacive dunites and pyroxene-rich lithologies, in both mantle peridotites and crustal intrusions, illustrate that local equilibrium was closely approached along the contacts (on a mm scale) in these settings.

Prior Work on Focused Flow in Partially Soluble Solid Media

This section is a brief summary of prior work on focusing of porous flow in partially soluble porous media. Chadam and coworkers [*Chadam et al.*, 1986; *Ortoleva et al.*, 1987] discussed formation of channels in partially soluble, porous rocks by infiltrating aqueous fluids. In a situation closely analogous to the experiments described in the second section of this paper, a planar dissolution front perpendicular to the flow direction is unstable and will break down into systematically spaced "fingers," provided a critical Peclet number is exceeded. *Hinch and Bhatt* [1990] provided a linear stability analysis similar to that of Chadam et al. but incorporating the width of a finite thickness reaction front. *Steefl and Lasaga* [1990] have advanced this theory with a series of analytical calculations and numerical simulations which provide insight into the factors controlling the length scales and aspect ratios of channels. They offered a simplified formulation for the Peclet number which must be exceeded for channeling instabilities to form

$$Pe = v_z L_x / D > \pi\,(3 - \Gamma)(1 + \Gamma)/[2\,(1 - \Gamma)]$$

where

$$\Gamma = \phi_i\,\kappa_i / \phi_f\,\kappa_f$$

in which v_z is the fluid velocity, L_x is a measure of the width of the system or between adjacent fingers, D is the diffusivity (including dispersion due to porous flow), and ϕ and κ are the porosity and permeability, with subscripts i and f indicating values before and after a dissolution reaction. As noted by both Chadam et al. and Steefl and Lasaga, channeling instabilities are possible for virtually any combination of v and D, provided that the width of the system is sufficiently large.

In addition, *Steefl and Lasaga* [1990] emphasize the importance of the reaction rate in determining the growth rate and morphology of dissolution channels. If reaction rate is much slower than v_z, for example, then small initial variations in porosity may not lead to instability. *Hoefner and Fogler* [1988] and *Daccord* [1987] have done laboratory experiments investigating the combined influence of dissolution reaction rate and flow velocity on the morphology of dissolution channels in porous media composed of natural and synthetic carbonates. They found that focusing of flow in dissolution channels is most pronounced at intermediate values of the ratio of reaction rate to v_z.

Tait and coworkers [*Tait and Jaupart*, 1991; *Tait et al.*, 1992] and *Bédard et al.* [1992] have investigated focusing of porous flow in solidifying crustal plutons, with experiments involving compositional convection in a cooling, crystallizing system. Experiments were conducted in tanks filled with aqueous ammonium chloride solutions. In these systems, cooled from below, liquids derived from crystal fractionation were less dense than hotter initial liquids and rose buoyantly from the base of the tank. Rising, evolved fluid was heated by its surroundings and became undersaturated with respect to the surrounding solids. As a consequence, upward flow of evolved liquid from the base formed "chimneys," regularly spaced cylindrical dissolution channels, in the accumulating crystal mush at the base of the tank. For reasons similar to those in our experiments, the ability of the rising fluid to dissolve part of its porous matrix led to focused channels for upward flow. By contrast, return flow of descending, cooling, crystallizing fluid in Tait et al.'s experiments was diffuse.

In the second paper in this series, *Tait et al.* [1992] showed that slower cooling of the system leads to formation of sheetlike, tabular dissolution channels, which are arranged in hexagonal arrays, as well as cylindrical tubes at the intersections of the sheets. This observation may be of fundamental importance in understanding tabular replacive dunites observed in the mantle section of ophiolites. However, we caution that the planar geometry of dissolution channels in Tait's experiments may be a consequence of the convective geometry of fluid in the tank, with limited applicability to ascent of melt through the upper mantle.

Finally, it is worth noting that the dissolution instability closely resembles an instability that happens when hot fluid with viscosity that decreases with temperature flows into a cool region [*Whitehead and Helfrich*, 1991]. In a manner similar to the dissolution channeling instability, fluid that flows faster stays hotter and less viscous than slow fluid. Theory indicates that the most unstable flow is in elongated channels. In addition, the inclusion of elasticity leads to periodic flow under some conditions.

Results of Laboratory Experiments

Dissolution Experiments

This section illustrates the results of some initial experiments which demonstrate the dynamic instability of diffuse porous flow in a soluble matrix. Table salt (NaCl) and 0.1 to 2 mm glass balls were combined into an approximately homogeneous mixture within a rectangular glass tank 58.3 cm high x 63.5 cm long x1.0 cm wide (Figure 4). Water was slowly fed from above through a pipe with many small holes to make the flow even. Water was maintained at a constant level above the solid matrix. The top of the salt and glass mixture was approximately planar, parallel to the top of the tank and perpendicular to the flow direction. The water descended through the salt and glass balls, dissolving salt until it became almost completely saturated. At the bottom, water escaped through a 3-cm layer of foam rubber above approximately 50 small holes in the bottom of the tank.

Porous flow rapidly became focused along salt-free dissolution channels parallel to the flow direction (Figure 5). Preliminary experiments [*Whitehead and Kelemen*, 1994] conducted using only salt, without glass balls, had qualitatively similar results. However, as dissolution channels formed, the top of the dissolving salt in the tank was gravitationally unstable and formed slopes which quickly reached the angle of repose of salt. Glass balls of variable size were introduced to hold salt grains in place in order to study the morphology of dissolution channels in a more rigid matrix. As proposed by Chadam and coworkers, flow is focused in growing dissolution channels because initial perturbations in porosity are magnified by dissolution of salt. Areas with slightly higher than average porosity have higher water/salt ratios resulting in lower salinity and rapid dissolution, and higher permeability permits faster ingress of water, undersaturated in salt, from higher in the chamber. Both these factors in turn lead

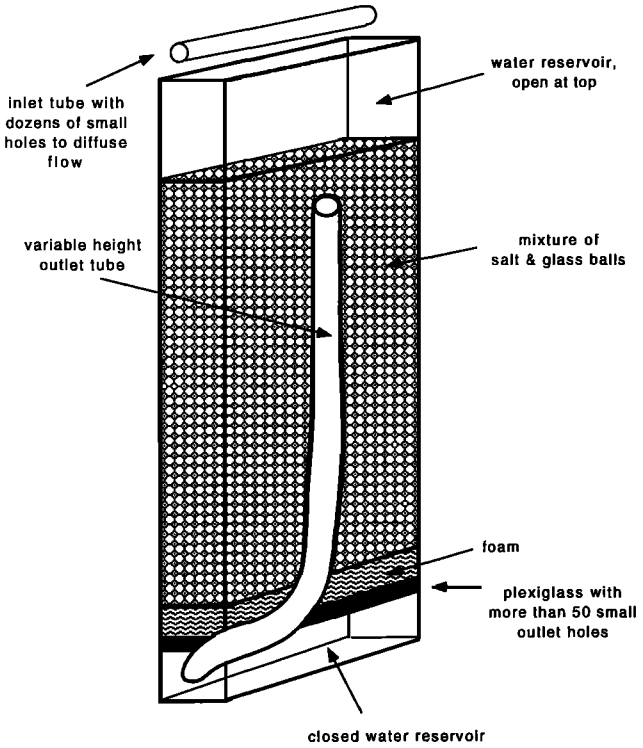

Figure 4. The tank used in experiments described in the second section. The outside walls and base are constructed of Plexiglas. Diffuse flow into the tank, more rapid than the out flow, fills a reservoir of water at the top. Excess input spills off the top of the tank. Water inside the tank runs down through a mixture of glass balls plus salt and descends through a layer of foam near the base, then through many small outlet holes, into a closed reservoir. The only outlet from this basal reservoir is via a tube whose height can be varied in order to control the total pressure in the tank.

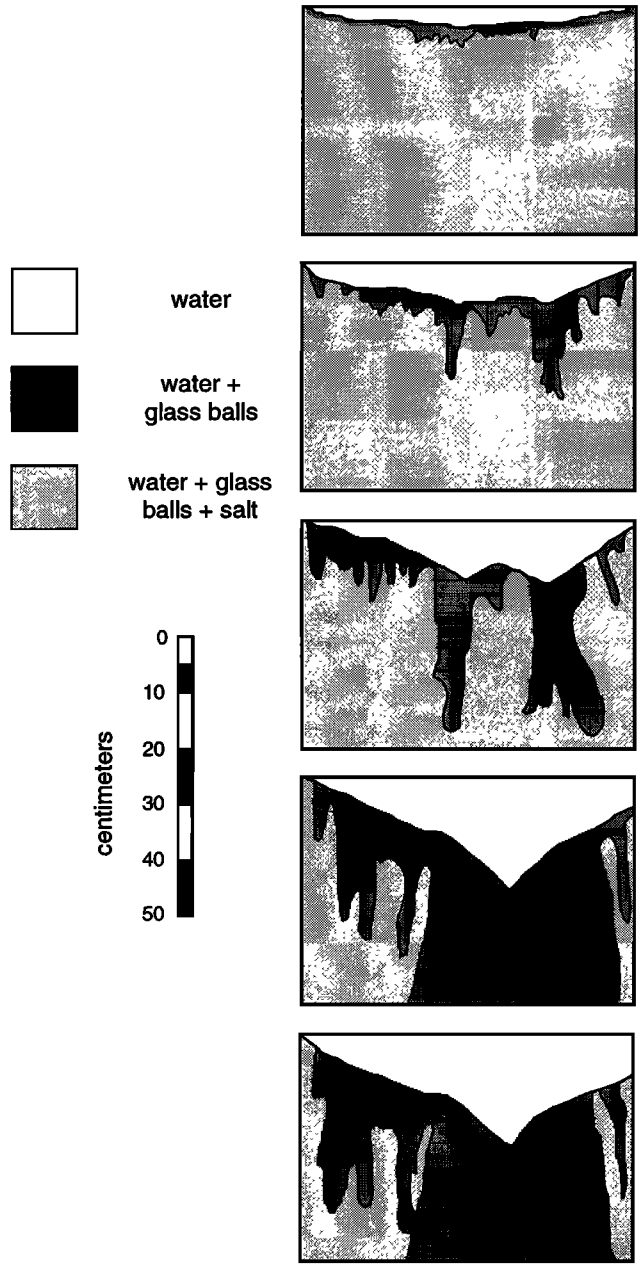

Figure 5. Results of an experiment in which water runs down through a mixture of glass balls and salt. An initially planar, horizontal interface is present between the water reservoir at the top of the tank and the mixture of glass balls and salt. As time progresses, descending water dissolves salt from the porous matrix. Within minutes, the planar dissolution front becomes unstable, and elongate dissolution channels parallel to the flow direction begin to form. In the initial stages of this process, many short channels form. As time progresses, the longer, wider channels increase in length very rapidly, while the smaller ones cease to grow and ultimately disappear as the solution front advances. Some compaction of the mixture of glass balls and salt occurs as the salt is removed by dissolution, and compaction is greatest above the largest dissolution channels.

to more rapid dissolution of salt in and above the region of high porosity, creating a channel with even higher average porosity, and so on.

The dissolution front remains a sharp boundary throughout the experiments, separating salt-absent porous media composed only of glass balls from salt-rich porous media with approximately the initial concentration of salt (as determined by visual inspection). This suggests that conditions of local equilibrium are very nearly maintained along the dissolution front; water flowing across the front becomes saturated in salt over a submillimeter scale. As the experiments progress, large dissolution channels grow at the expense of nearby, smaller ones, resulting in formation of a series of regularly spaced "hills" and "valleys" in the dissolution front. With time, the amplitude of the larger channels increases, and the number of channels decreases, so that only a few channels extend to the bottom of the chamber at the end of the experiment. This occurs because relatively high permeability within the large channels leads to relatively low hydrostatic pressure at their tops. This, in turn, leads to lateral flux of water into the tops of larger channels. Additional flux of water through the large channels leads to their continued growth, while decreased flux in smaller, adjacent channels leads to their disappearance as the dissolution front advances through the tank.

A second important observation from these experiments is that flow lines for fluid in the salt/glass matrix converge toward dissolution channels near their upstream ends and diverge from dissolution channels near their growing, downstream ends (Figure 6). Relatively low hydrostatic pressure at the upstream end of a high-porosity dissolution channel leads to lateral influx. High flux

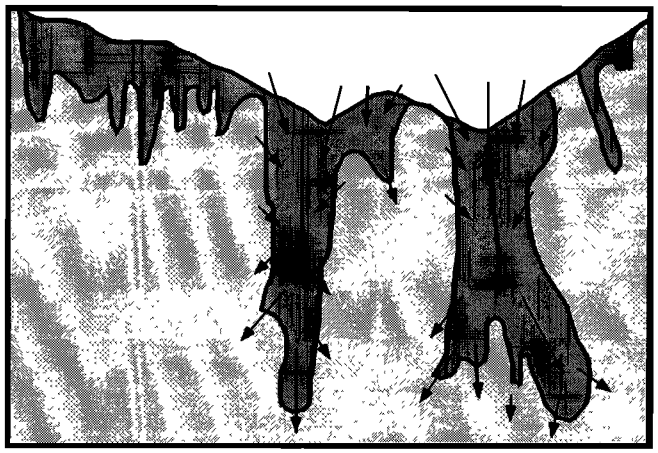

Figure 6. Flow vectors at one time during the experiment illustrated in Figure 5 Flow lines converge toward dissolution channels near their tops and diverge from the center of dissolution channels near their bases. The approximate direction and relative magnitude of fluid velocity indicated by the vectors were determined by observing the distribution of dye injected along the top of the tank during the experiment.

within the channel, in turn, causes high hydrostatic pressure at the downstream end (the channel "tip") where permeability decreases, resulting in lateral dispersion of flow out of the channel. If applicable to the mantle, this observation has the potential to resolve the paradox noted by *Carlson* [1992], in which there is geochemical evidence for flow of magma toward some dunite channels [e.g.,*Takahashi*, 1992], while other dunite channels show evidence of outward flow [e.g., *Kelemen et al.*, 1992].

The length of the channels (measured from the upstream limit of the dissolution front in the tank) can be fitted as an exponential function of time (Figure 7). An initial exponential growth rate is in accord with the linear stability analysis of *Chadam et al.* [1986], who considered the channeling instability in a porous medium with a two-dimensional flow field. Here we present a simplified version of this stability analysis in order to illustrate some of the essential physics of the process. A liquid flowing uniformly in a porous material encounters a material of lower permeability which it can partially dissolve. The dissolution restores the material to the original permeability. The interface between the two materials is initially flat, and extends at right angles to the flow. The stability of the flat interface, and the spatial distributions of permeability, porosity, solute concentration, and water composition were studied by *Chadam et al.* [1986] and *Ortoleva et al.* [1987]. They found that the planar interface is unstable with fastest growing wavelength determined by "grain size, initial modal amount of material reactive mineral in the rock, initial porosity and composition and velocity of the inlet fluid." Essentially, their mathematical relation simplifies to the wavelength of fastest growth being proportional to thickness of the front, which is determined by diffusivity divided by fluid velocity (within the "transport controlled regime" where reaction rate is almost as large as fluid velocity; for details, see *Steefl and Lasaga* [1990]). Since diffusivity of a solute flowing through a granular material is dominated by mechanical dispersion, which is equal to velocity times grain size [*Phillips*, 1991], this reduces to the simple fact that channel size is proportional to grain size.

Here, the essentials of such stability analysis are presented in as simple form as possible. For this purpose, many of the elements included by Chadam and coworkers, such as grain size,

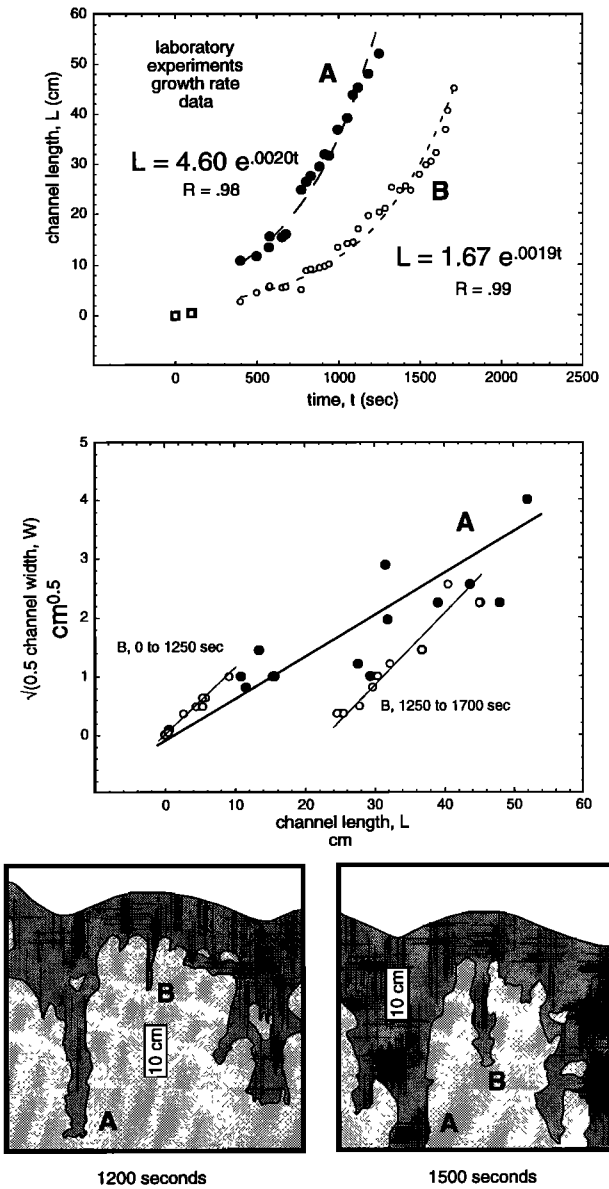

Figure 7. Length and aspect ratios of two dissolution channels in an experiment similar to that illustrated in Figure 5. Length is measured from the highest point on the dissolution front to the bottom of each channel. Channel A was the first to reach the bottom of the tank in this experiment, and B was the last discrete channel to reach the bottom. The growth of the channels can be fitted with an exponential function of time, as predicted in linear stability analysis by *Chadam et al.* [1986], and in the second section of this paper. The width of growing channels is approximately proportional to the square root of their length. Channel B shows two aspect ratio regimes, one developed before Channel A reached the bottom of the tank, and the other afterward. *Steefl and Lasaga* [1990] noted that growth of channels with width $\geq \sqrt{2}L$ minimizes the effect of lateral diffusion of solute into the growing finger. Bottom diagrams show channel morphology in this experiment after 1200 and 1500 seconds had elapsed.

porosity variation, change in volume of the solute, etc., will be neglected.

Let the interface lie at

$$\eta(x,t) = z \qquad (1)$$

and the equation for the dissolution of the interface be

$$\frac{\partial \eta(x,t)}{\partial t} = \gamma w \tag{2}$$

where w is flow velocity and γ is the ratio of the solubility to the concentration of the solute in the solid phase across the interface. In this model, the interface is immediately dissolved with a rate proportional to the amount of material flowing into the interface.

Let the total vertical velocity w consist of a steady, uniformly moving component plus a small perturbation, and let the interface consist of a flat horizontal plane plus a small deviation. These are expressed as

$$w = w_0 + w'(x,t).$$
$$\eta = \eta_0(t) + \eta'(x,t). \tag{3}$$

The steady flow and the flat interface are given by

$$\frac{\partial \eta_0}{\partial t} = \gamma w_0 \tag{4}$$

$$\eta_0 = \gamma w_0 t = z. \tag{5}$$

The behavior of the deviations from this flow will now be investigated. The equations governing perturbations to the liquid flow in the porous material are given by Darcy's law:

$$\frac{k_n}{\mu}\frac{\partial p_n}{\partial x} = -u_n$$
$$\frac{k_n}{\mu}\frac{\partial p_n}{\partial z} = -w_n$$
$$u_n = \frac{\partial \psi_n}{\partial z} \tag{6}$$
$$w_n = -\frac{\partial \psi_n}{\partial x}$$

so

$$\nabla^2 \psi_n = 0 \tag{7}$$

Here, subscript n=1,2 denotes the region upstream or downstream of the interface, respectively. Consider a perturbation to the interface

$$\eta' = N(t)\cos(lx). \tag{8}$$

We are seeking the lateral pressure variations due to the perturbed interface. Assuming $w_0 >> w'$, $t = 0$ (so the unperturbed interface is at $z = 0$) and $N(t)$ is smaller than the length scale, $2\pi / l$, integrate the equation for w upward from a plane normal to the bottom of the perturbed interface at z=-N to a plane normal to the top of the perturbed interface at z=N

$$p(-N) = -\frac{\mu}{k_1}\int_{-N}^{-\infty} w_0 dz = \text{const}. \tag{9}$$

Pressure from perturbation velocity w' is of order $w' N$ and is assumed to be negligible. The term in the left brackets is the pressure change that would be found even without the perturbation, and the one on the right is due to the perturbation. A boundary condition of y is produced using the x derivative of the pressure change from equation (9) along with the first equation of (6), and the fact that

$$p(-N) = -\frac{\mu}{k_1}\int_{-N}^{-\infty} w_0 dz = \text{const in x},$$

so that

$$\left.\frac{\partial p}{\partial x}\right|_{z=N} = -\mu w_0\left[\frac{1}{k_1} - \frac{1}{k_2}\right]\frac{\partial \eta'}{\partial x} = -\frac{\partial \psi}{\partial z}. \tag{10}$$

Since N is small, this condition will be assumed to apply at z=0. A solution to equation (7) is

$$\psi = A(t)\sin(lx)e^{-lz} \tag{11}$$

which produces with (8) and (10) at $z = 0$

$$A(t) = \mu w_0\left[\frac{1}{k_1} - \frac{1}{k_2}\right]N(t) \tag{12}$$

Using (2) with (4), (6), (8), (11), and (12) results in

$$\frac{\partial N}{\partial t} = -\gamma l w_0\left[\frac{1}{k_1} - \frac{1}{k_2}\right]N = \gamma l w_0\left[\frac{k_1 - k_2}{k_1 k_2}\right]N \tag{13}$$

which has an exponentially growing solution for $k_1 > k_2$ (upstream permeability greater than downstream),

$$N \propto e^{\gamma l w_0 [\frac{k_1 - k_2}{k_1 k_2}]t}. \tag{14}$$

Equation (14) shows that the larger the wavenumber, l, the faster the growth rate. Therefore, where we neglect diffusion and grain size, very small length scale perturbations initially grow most rapidly. The more complete theories of *Chadam et al.* [1986] and *Ortoleva et al.* [1987] have shown that diffusion processes and grain size limit the magnitude of the fastest growing wavenumber, so that fastest growth is scaled by grain size. In accord with this theory, the first wavelengths observed in our laboratory experiments are small, but larger than grain size. The disappearance of the short wavelength channels later in the experiments is probably a result of lateral entrainment of flow into the longer wavelenth channels.

These results, and those of Chadam and coworkers, are for growth at infinitesimally small channel length and not directly applicable to the finite channels measured in experiments described here. Nonetheless, approximate values from the experiment in Figure 7 are used in the following calculation. Given solubility of NaCl in water at 25°C of about 0.2 (weight units) and concentration of NaCl in the initial solids of about 0.4 (so that $\gamma = 0.5$), width of the box of about 50 cm ($l = 2\pi/50$), an initial flow velocity of 0.05 cm/s, and a final flow velocity of 0.5 cm/s (such that $k_1 = 10\,k_2$), one obtains

$$N \propto e^{0.003t}$$

in surprisingly close agreement with the observed growth rates of finite channels in the experiment. The agreement between the prediction for growth of infinitesimally small channels with our data for growth of finite channels suggests that the channel length remains unstable throughout the experiments.

Our experimental results on growth rate are different from those in the numerical experiments of *Steefl and Lasaga* [1990]. They studied a system of fixed width, with an initial high-porosity channel about half as wide as the system, and found that the length of the channel initially increased as an exponential function of time but that the growth rate subsequently decreased. Factors which could limit the length of dissolution channels as they grow include (1) lateral diffusion of the solute into the growing channel and (2) limitations to the lateral entrainment of flow due to fixed system width. In considering (1), it is apparent that diffusion of salt into the water within a very long, narrow channel will eventually result in a decreasing dissolution rate at the tip of the channel. However, Steefl and Lasaga note that increasing width of growing channels, so that the square of the half width is proportional to the length, would preserve the initial ratio of transport time down the channel to diffusion time across the channel, neutralizing the negative feedback effect of lateral diffusion in a long, narrow channel. Figure 7 illustrates that these dimensions were generally maintained during channel growth in our experiments. This was not possible in Steefl and Lasaga's simulations, beyond a certain point, because of the limited width of the system. Factor (2) may also have affected their results. These limitations were unimportant at the flow velocities and length scales of the experiments described in this paper, and may not be present in any system with semi-infinite width.

Crystallization Experiments

This paragraph briefly describes preliminary experiments investigating the morphology of porous flow when liquid mass is decreasing, and solids are precipitated. Water saturated in ammonium chloride, at room temperature, was released through a central hole into a narrow gap (~1.4 mm) between a leveled, circular aluminum plate maintained at 0°C and an overlying Plexiglas plate. The ammonium chloride solution flowed radially outward to the free edges of the plates. As in the porous flow experiments described above, the hydrostatic pressure was held constant in these experiments by maintaining a constant level in the reservoir of ammonium chloride solution. The solubility of ammonium chloride in water is strongly temperature dependent. Upon contact with the cold aluminum plate, the saturated solution began crystallizing ammonium chloride as it cooled and flowed radially outward. Crystals thus began to fill the "porosity" between the aluminum and Plexiglas plates, restricting flow. Figure 8 schematically illustrates the results. Whereas flow is initially diffuse and radial, it very quickly is restricted to a single channel, which becomes armored with crystal-rich "walls." Initial flow focusing occurs because channels with rapid fluid flux cool and crystallize less than fluid undergoing radially dispersive flow. However, the solution flowing through the initial channel still cools as it passes outward and so continues to crystallize. Crystallization ultimately restricts flow so that the channel is no longer the most permeable path for fluid introduced at the center of the plates. At this point, most of the flow begins to pass through a relatively high-porosity section of the channel wall, forming a new channel. This sequence of events is periodically repeated throughout the duration of the experiments. In some experiments, the transition from one channel to another is precipitated by formation of brittle cracks in the initial channel wall.

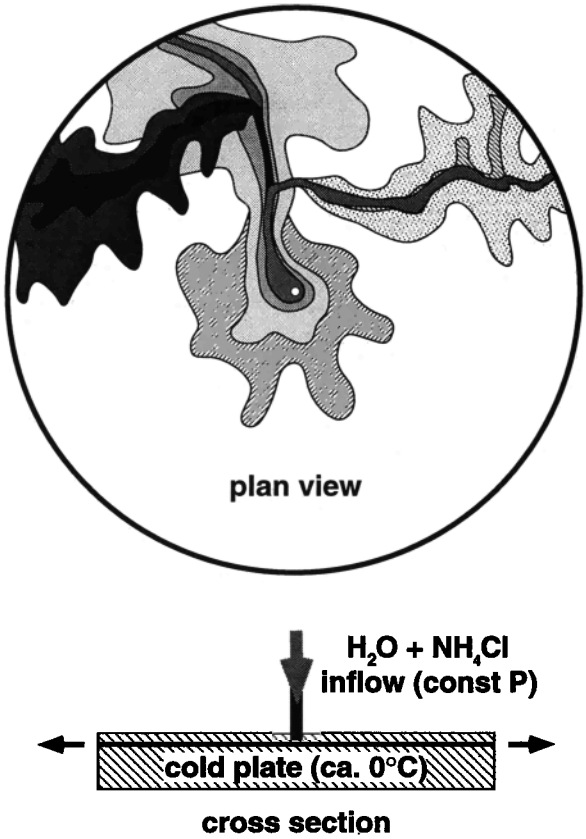

Figure 8. Schematic illustration of results of experiments in which an aqueous solution, saturated in ammonium chloride at room temperature, is injected into a narrow gap between two circular plates, as illustrated in the bottom diagram. Liquid is injected at the center and flows outward, escaping from the free edge at the perimeter of the plates. The lower plate is maintained at 0°C, which causes cooling of the solution and crystallization of ammonium chloride. At the top is a "stratigraphic" map of the distribution of ammonium chloride crystals over time. Later flow paths are superimposed on those which formed earlier. In all experiments, initially radial flow of fluid quickly organizes itself into a single channel of focused flow. This channel is surrounded by porous "walls" of ammonium chloride crystals. Flow in a channel permits outward flow of fluid with a minimum of cooling and crystallization. Eventually, however, interior crystallization "chokes" the channel. Sometimes, increasing pressure in the channel leads to cracking in the wall. After the channel "chokes," flow is diverted through a high-porosity region or a crack in the channel wall. Release of the fluid into a relatively crystal-poor areas is followed by initially diffuse flow, then by formation of another walled channel, and so on.

Results of Numerical Experiments

Numerical experiments on formation of dissolution channels have been made using a modification of the "lattice gas" model first proposed by *Frisch et al.* [1986]. Lattice gases are fully discretized models of molecular dynamics, in which an ordered lattice is populated by identical, pointlike particles positioned on the nodes. The particles propagate along the lattice links, "hop"

one node per time step, and interact with each other only when they meet at a node. Then a collision occurs, conserving mass and linear momentum. After the collision the particles are redistributed in the available lattice directions. In the limit of small velocities, the behavior of individual particles, taken as a whole, leads to macroscopic behavior that resembles the flow of fluid. Equations describing the macroscopic behavior of the lattice gas closely resemble the incompressible Navier-Stokes equations. Lattice gases are especially useful in treating complicated boundary conditions such as flow through porous media, because one need not solve the Navier-Stokes equations at the boundary: one merely lets the particles bounce off it [e.g., *Rothman*, 1988]. To simulate a pressure gradient, one increases the probability that particles will move in a specified direction. By controlling the collision rules, one can also vary viscosity and diffusivity [e.g., *Henon*, 1987; *d'Humiers et al.*, 1988].

Simulations in this paper use a floating point analog of the lattice gas method (the relaxation lattice Boltzmann method of *Qian et al.* [1992]), allowing mixtures of miscible fluids [*Flekkoy*, 1993], to which chemical dissolution and precipitation were added [E. Aharonov, manuscript in preparation]. In order to simulate a liquid dissolving the porous media through which it is flowing, one gives the fluid particles the ability to detach solid particles from a wall upon colliding with it. The probability of detaching a solid particle is

$$P = (1\text{-}C/C_{eq})[(n - s)/n]$$

where C is the concentration of the solute in the fluid, C_{eq} is the equilibrium concentration of the solute in the fluid, and the final term is a surface tension or chemical potential gradient effect which prevents "tunneling" into aggregates of solid particles, wherein n is the total number of nearest neighbors on the lattice (6 for the two-dimensional hexagonal lattice), and s is the number of solid nearest neighbors. The probability of detaching a solid particle decreases as the concentration in the fluid rises, until a saturation level is reached and no more dissolution occurs. This numerical technique allows one to vary both the diffusivity and the reaction rate, thus probing into the transport-controlled, diffusion-controlled, and reaction-controlled regimes [e.g., *Hoefner and Fogler*, 1988; *Steefl and Lasaga*, 1990].

Experiments With a Solution Front and No Gradient in Solubility

This section is a description of results of numerical experiments closely analogous to our salt dissolution experiments. An initially undersaturated "fluid" flows between regularly spaced grains of "salt." Initially, one salt grain in the upper row is missing. As predicted by *Chadam et al.* [1986] and *Steefl and Lasaga* [1990], no instability is observed in these experiments until a critical Peclet number is exceeded. The critical Peclet number may be reached by decreasing the diffusivity, or increasing the pressure gradient, and thereby the initial flow velocity. Above the critical Peclet number, an elongate channel grows parallel to the flow direction. Figure 9 illustrates the flow field in the fluid after the channel has propagated about halfway through the experimental box. Fluid flows laterally into the dissolution channel near the upstream end and laterally out of the channel near the downstream end, as observed in channels in the water and salt experiments described in the second section of this paper. The length of the channel can be approximately fitted as an exponential function of time, as shown in Figure 10.

Experiments With a Gradient in Solubility and No Solution Front

The initial condition in the experiments described in the previous section is one in which there is a concentration front in the solid matrix. Upstream of this front, there are no soluble solid particles. In the mantle, by contrast, the porous medium is initially composed of homogeneous peridotite. Partial melts are initially saturated in all solid phases. As melts ascend, they become undersaturated in solids. This undersaturation will drive dissolution reactions which tend to restore equilibrium, but at the same time the dissolution process may produce a channeling instability. If high-permeability channels form, higher flow velocities will drive liquids away from equilibrium, in turn increasing the dissolution rate and leading to faster channel growth.

Figure 11 illustrates the results of a numerical experiment in which the incoming fluid is saturated in the solid matrix phase, but there is a gradient in solubility, so that the equilibrium concentration of the solute in the fluid increases downstream. Despite the absence of a solution front in this experiment, a channeling instability is observed. This illustrates that dissolution channels may nucleate and grow in a homogeneous medium (such as may be found in the upper mantle), in the absence of an initial solution front. A full linear stability analysis of this problem, incorporating the effects of compaction in a viscously deforming solid matrix, has recently been completed [*Aharonov et al.*, 1994, Channeling instability of upwelling melt in the mantle, submitted to *Journal of Geophysical Research*, 1994]. The analysis confirms that diffuse porous flow of melt in the adiabatically upwelling mantle is unstable and will form high-porosity channels that are elongate in the vertical dimension.

The numerical experiments also illustrate another consequence of having a gradient in solubility. Because a new instability can nucleate anywhere within a continuous porous medium, in the presence of a gradient with solubility increasing downstream, there may be no limiting length for growing dissolution channels, even if the width of the system is limited. Dissolution channels in the mantle could span regions in which liquids ascend by porous flow along a nearly adiabatic PT gradient. This may apply to most of the melting regime beneath mid-ocean ridges.

Discussion

Channels in the Mantle

Formation of dissolution channels as a result of the reactive infiltration instability is likely during adiabatic ascent of melt in the upper mantle, provided that advective flow rates are substantially greater than diffusion and dispersion in migrating liquids so that a critical Peclet number is exceeded. The fact that dissolution channels are observed as replacive dunites, at the centimeter to 100-m scale in outcrops of shallow mantle peridotite, indicates that this critical Peclet number is exceeded in the mantle at some times and places. The time scales and length scales for the channeling process remain uncertain. On the basis of results of the experiments on the channeling instability in a solubility gradient, as well as our recently completed linear stability analysis for this problem, incorporating the effects of compaction [*Aharonov et al.*, 1994, submitted manuscript, 1994], it is inferred that diffuse porous flow may be unstable throughout regions in the upper mantle where liquid ascends along an adiabatic PT gradient. In these regions, the solubility of mantle silicates in the initial liquid increases along the ascent path. Perturbations in

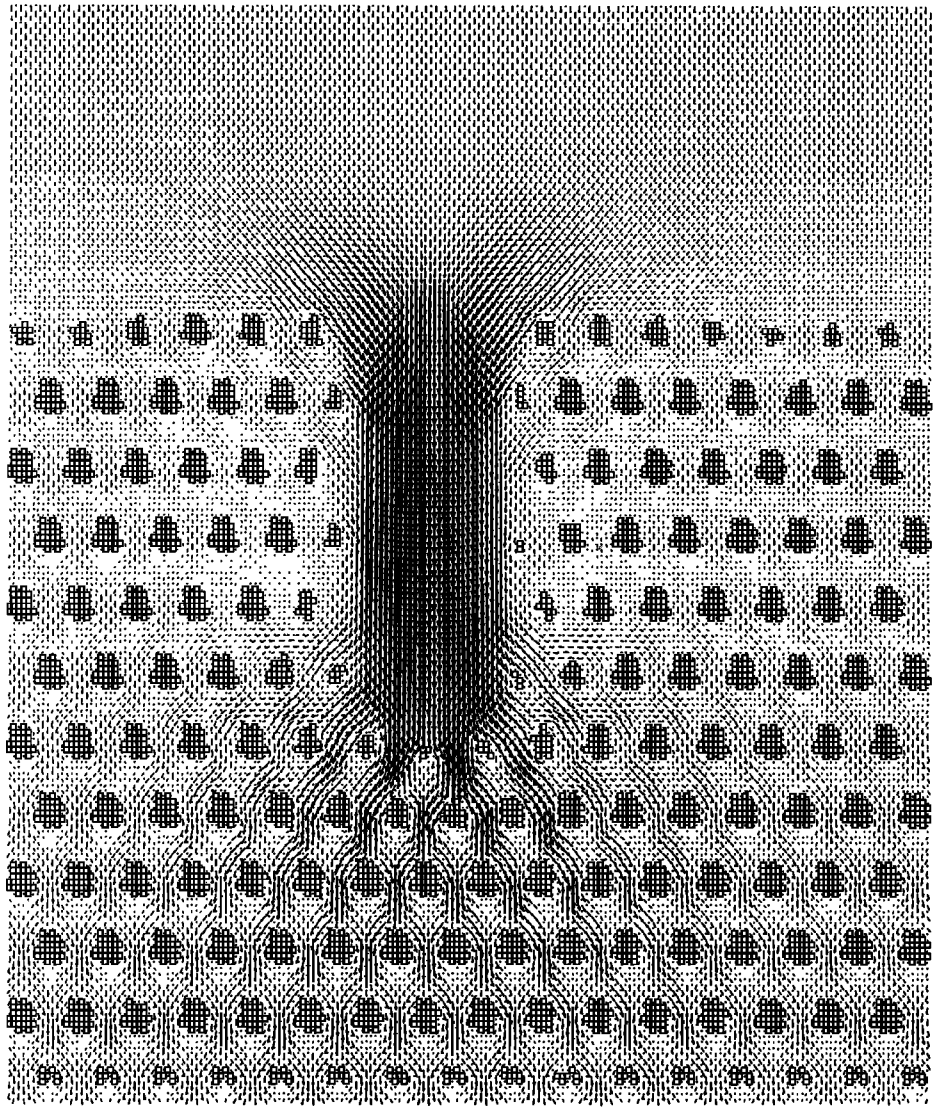

Figure 9. Results of a numerical experiment using a modified relaxation Boltzmann Method [*Qian et al.*, 1992; *Flekkoy*, 1993; *E. Aharonov*, manuscript in preparation, 1994]. Fluid particles enter the box at the top and exit at the bottom. The pressure drop across the box is constant. Open squares indicate the position of solid particles. Fluid enters the top of the box with a solute concentration of zero and gradually dissolves solids (see text). Arrows illustrate the direction and magnitude of fluid velocity. Initially, the box holds a regular pattern of solid particles, except for one missing square group of particles in the top row. This figure illustrates the configuration of the system in an experiment with high Peclet number after a dissolution channel has grown about halfway down the box. There is lateral flow of fluid into the top of the channel, and lateral flow out of the base of the channel, as in results of experiments on water flowing through mixtures of glass balls and salt (see Figure 6).

porosity anywhere along such an ascent path may be sufficient to initiate formation of channelized flow. The tip of a growing dissolution channel will itself be unstable, and porous channels should continue to grow throughout the region of adiabatic ascent.

At this juncture, the effect of compaction should be addressed. As shown by *McKenzie* [1984], the rate of extraction of melt from a porous network is limited by the rate of compaction of the solid matrix. In the mantle, compaction is a ductile process, limited by the viscosity of the solid phases. During isochemical compaction, per se, the melt fraction in the system remains fixed. The compaction scenario must be modified for systems in which the mass of melt is changing. Two opposing factors must be considered: (1) the effective viscosity of the solid matrix decreases as the melt fraction increases, so that compaction may proceed more rapidly in regions of high porosity, and (2) for a constant pressure drop across the system, flow velocity, fluid flux, and dissolution rate all increase in more permeable areas, so that increasing porosity due to dissolution reactions will be more rapid in regions of high porosity.

Compaction is unlikely to retard the initiation and growth of dissolution channels for three reasons. First, compaction in geologically reasonable times cannot occur over distances smaller than a characteristic "compaction length," often estimated to be 100 m to 1 km in the upper mantle [e.g., *Spiegelman*, 1993]. Thus high-porosity channels can grow to at least these lengths

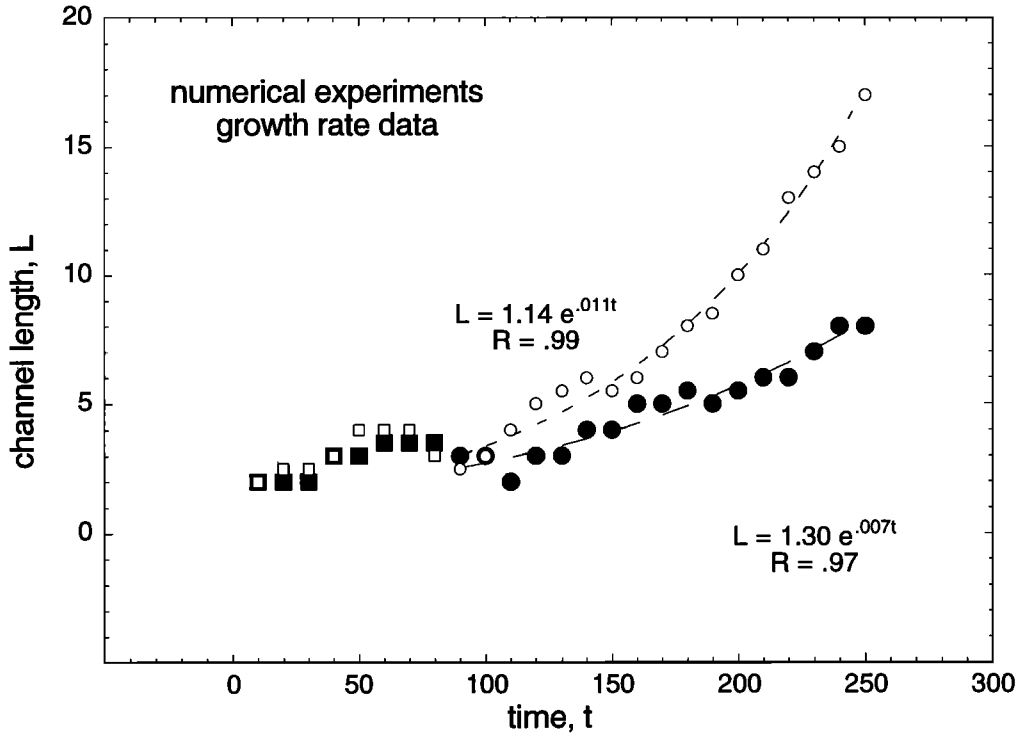

Figure 10. Length of dissolution channels in numerical experiments, measured from the highest remaining solid particle to the bottom the channel, as a function of time. Initially, measurement of the length is complicated by the wide spacing of the solid particles in the vertical dimension. As the growth of the channel proceeds, a more smooth and accurate measurement can be made. As for experiments on water flowing through mixtures of glass balls and salt, the growth of the channels can be fitted with an exponential function of time, as predicted in the linear stability analysis of *Chadam et al.* [1986] and in the second section of this paper. Fitted values are illustrated as circles, those which were excluded from the fit are shown as squares. Solid symbols are for the experiment illustrated in Figure 9, in which there is an initial solution front and no gradient in the saturation concentration of the solute in the fluid. The saturation concentration was 0.05. Open symbols are for an otherwise identical experiment in which the saturation concentration varied linearly as a function of vertical position, from 0.05 at the top to 0.1 at the bottom.

without being "squeezed closed" by compaction. Second, since compaction of partially molten peridotite by two phase flow may proceed linearly with time under some circumstances [e.g., *McKenzie*, 1984], it may be slower than exponential growth of dissolution channels. In other words, silicate dissolution rates of microns to centimeters/day under geologically reasonable conditions [e.g., *Kuo and Kirkpatrick*, 1985; *Brearley and Scarfe*, 1986; *Zhang et al.*, 1989] may be much faster than viscous flow of solids in compaction. Third, the presence of an interconnected column of liquid, of the order of one compaction length or more, may lead to magmatic overpressure near the top of a growing channel and drive decompaction rather than compaction. Our recently completed linear stability analysis of the reactive infiltration instability in a solubility gradient, including the effects of compaction, [*Aharonov et al.*, 1994, submitted manuscript, 1994], demonstrates that diffuse porous flow of melt in the mantle is unstable - even on length scales greater than a compaction length - and will break down into long, narrow porous channels (in two dimensions).

Formation of cracks or melt-filled lenses could limit the growth of channels under some conditions. Brittle fracture of adiabatically upwelling mantle peridotite may be unlikely, since asthenospheric peridotite deforms viscously and is generally thought to be too weak to support stresses sufficient to form cracks. However, decompaction into melt-filled lenses, as envisioned by *Sleep* [1988, submitted manuscript, 1994], may be a natural consequence of increasing porosity and permeability within a dissolution channel. Once such lenses form, they may tap much of the liquid in the system, removing it from the porous flow regime and forestalling the continued growth of dissolution features.

There are numerous uncertainties regarding the long-term fate of dissolution channels once they form. Continuing dissolution of mantle olivine, in adiabatically ascending liquid within a dunite channel, could, in principle, create open tubes or lenses, filled only with liquid, solely as a result of dissolution reactions where the melt/rock ratio becomes very high. Formation of open space in this manner could account for the presence of "cumulate" chromitite bodies within dunites in shallow mantle peridotite. Because of the very limited solubility of Cr in basaltic magmas, the presence of chromitites is indicative of chrome spinel crystallization from an enormous volume of basaltic liquid within a very small space in the shallow mantle [e.g., *Leblanc and Ceuleneer*, 1992]. However, compaction processes are likely to play an important role in limiting the size and duration of such features.

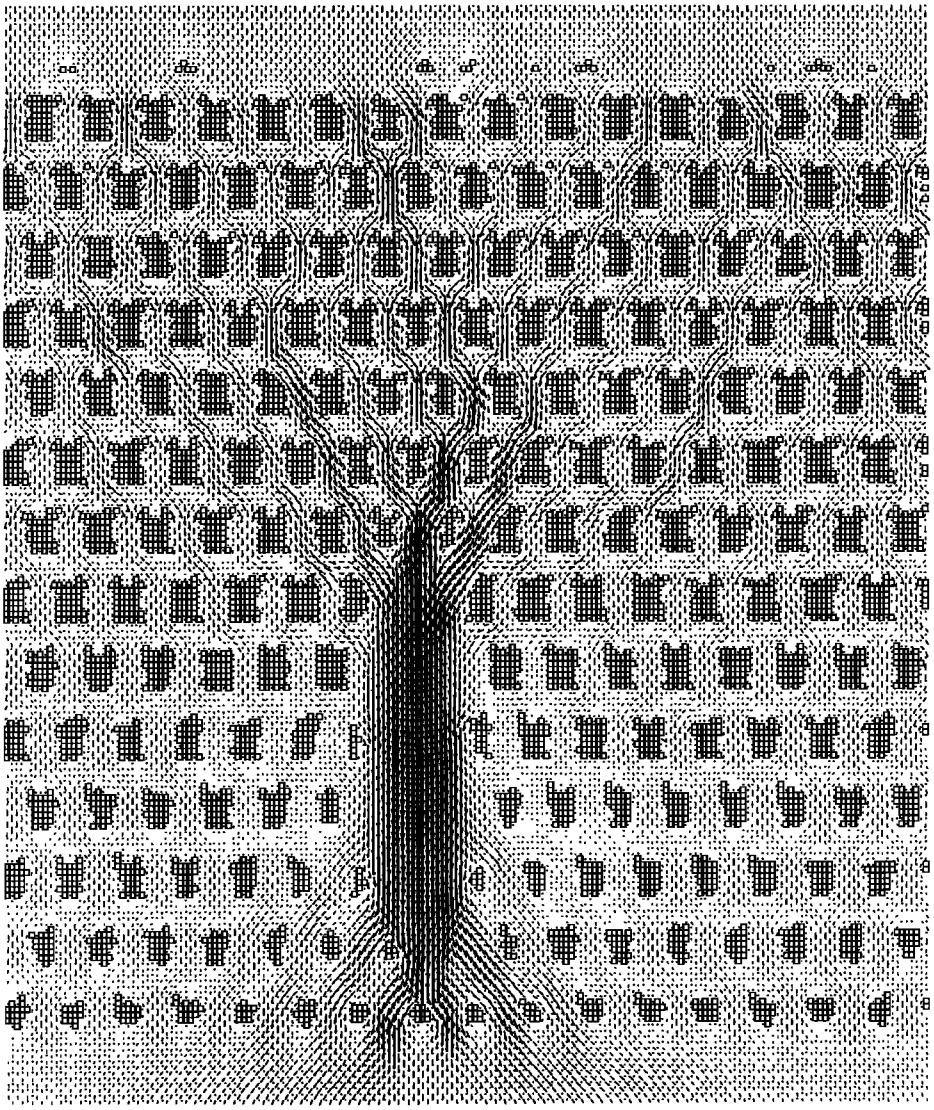

Figure 11. Results of a numerical experiment similar to that illustrated in Figure 9, except that here the saturation concentration of the soluble material in the fluid varies from zero at the top of the box to 0.05 at the bottom. Initially, the box held a regular pattern of solid particles, except for one missing group of particles in the ninth row from the top. This figure illustrates the configuration of the systems after a dissolution channel has begun to grow from the position of the missing solid particle. As in Figure 9, squares show the position of solid particles, and arrows indicate the direction and magnitude of flow velocity. It is inferred from these results that diffuse fluid flow in a soluble porous medium is unstable even in the absence of an initial solution front in the system and will form channels where fluid becomes gradually undersaturated in solids downstream. This result has recently been confirmed by linear stability analysis [*Aharonov et al.*, 1994, Channeling instability of upwelling melt in the mantle, submitted to *Journal of Geophysical Research*, 1994].

Flow of Cooling Melt in Mantle on a Conductive Geotherm

Ancient, subcontinental mantle "tectosphere" [e.g., *Jordan*, 1988] is essentially static and must be close to a conductive geothermal gradient. Where melt ascending by porous flow encounters the tectosphere, it must begin to cool . Such cooling liquids will become saturated in solid phases and decrease in mass, but it does not follow that they will crystallize within a narrow depth interval. On the contrary, volatile and incompatible elements, such as H_2O, CO_2, and K_2O, will be concentrated in the gradually crystallizing liquid, lowering the solidus temperature and viscosity of the evolving liquid. Whereas the liquidus temperature of a (nearly) anhydrous basaltic magma at 2 GPa may be 1400°C, the solidus temperature for the last fraction of hydrous liquid derived by very slow, fractional crystallization of such a basaltic magma along a geotherm with an average slope of 5°C/km may be less than 900°C, at a level 10 km higher . Thus extensive portions of the tectosphere may be traversed by cooling magmas, migrating by porous flow and decreasing in mass as a result of crystal fractionation. Under these circumstances, it is expected that transient conduits will form, armored by low-permeability walls formed by crystallization. Porosity in these conduits will eventually be choked with newly crystallized material. When one conduit is choked, focused flow of magma will

migrate elsewhere so that on large scales of time and distance, porous flow of melt in such settings will be essentially random and diffuse. This hypothesis is supported by experiments on channel formation in convecting, crystallizing ammonium chloride solutions [*Tait and Jaupart*, 1991; *Tait et al.*, 1992; *Bédard et al.*, 1992], who observed that where fluids in their experiments are heating and dissolving solids, porous flow is focused, whereas where fluids are cooling and precipitating additional solid material, porous flow is diffuse.

An interconnected melt network in the asthenosphere, in the zone of focused flow, may develop a substantial hydrostatic head. Above, where the interconnected melt network becomes clogged with crystals due to magmatic cooling, there may be a substantial hydrostatic overpressure. Under these circumstances, cracks may form due to hydrofracture, and melt may be periodically expelled in dikes, in a process similar to that proposed by *Nicolas* [1990]. Similarly, increasing volatile contents of evolving magmas, combined with decreasing pressure, may result in volatile saturation, expansion of the liquid+gas system, and hydrofracture. In shallow mantle sections in ophiolites, this may explain why dunites generally form anastomosing, replacive features indicative of melt migration by porous flow, whereas pyroxenites and gabbroic rocks, which crystallize from cooling magmas, almost always form narrow, tabular dikes [e.g., *Kelemen and Dick*, 1994].

Geochemical Consequences of Flow in Channels

Very different porous flow morphology and chemical consequences may be anticipated for melt extraction in different geodynamic environments. As illustrated in Figure 12, beneath mid-ocean ridges, both liquids and solid peridotite ascend along a nearly adiabatic pressure-temperature trajectory, almost to the base of the crust. Beneath hot spot volcanoes, ascending mantle (and partial melt) follows an adiabatic ascent path to the base of the tectosphere, but at shallower levels, melts must pass through conductively cooled mantle. Thermal models of subduction zones indicate that an inverted geotherm must form above the cold, subducting slab [e.g., *Peacock*, 1991; *Davies and Stevenson*, 1992]. Liquids generated in or above the subducting slab must initially heat as they rise through this inverted geotherm [*Kelemen*, 1990, 1994; *Kelemen et al.*, 1993]. After liquids pass through the thermal maximum in the mantle wedge, they must ascend through cooler mantle to reach the surface.

Beneath a mid-ocean ridge, liquid mass and porosity will continually increase through most of the mantle decompression path, both by addition of partial melts from decompressing peridotite and as a consequence of the dissolution reactions discussed in this paper. If porous flow begins to organize into dissolution channels, this process is likely to run away and to continue almost to the base of the crust. Consequently, melt will flow primarily through dunite conduits, melt/rock ratios within conduits will be very high, and the chemical effects of melt/rock reaction will be subdued in liquid products which form the oceanic crust. These inferences are schematically illustrated in Figure 13. This mechanism can explain the development of chemically isolated channels for rapid melt migration, whose existence has been postulated in order to explain the observed disequilibrium between mid-oceanic ridge basalts and residual, abyssal peridotites [e.g., *Spiegelman and Kenyon*, 1992; *Hart*, 1993].

Beneath both hot spots and arcs, liquids pass into conductively cooled mantle and will themselves begin to cool and crystallize. The interval over which such magmas may continue to ascend by porous flow may be tens of kilometers. Within this interval, they may form, fill, and abandon conduits with relatively impermeable walls. In this process, they may choke porosity forming impermeable caps, hydrostatic overpressure, and crack formation, as illustrated in Figure 14. Such a flow structure will produce increasingly small melt/rock ratios upsection, maximizing the

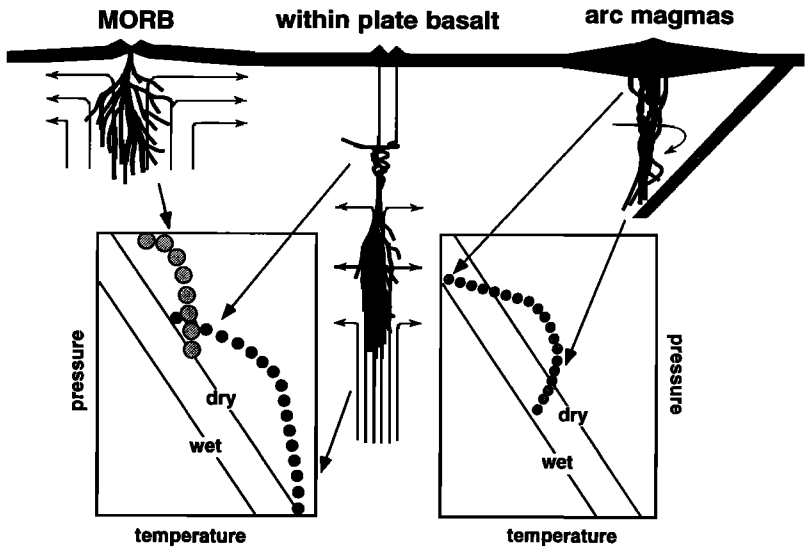

Figure 12. Geotherms and likely structure of porous flow channel networks in different magmatic environments. Beneath mid-ocean ridges, both liquids and solid peridotite ascend along a nearly adiabatic pressure-temperature trajectory, almost to the base of the crust. Beneath hot spot volcanoes, ascending mantle and partial melt follow a nearly adiabatic ascent path to the base of the tectosphere, but at shallower levels, melts must pass through conductively cooled mantle. In subduction zones, an inverted geotherm must form above the cold, subducting slab, and liquids generated in or above the slab must initially heat as they rise. After liquids pass through a thermal maximum they will cool as they continue to rise.

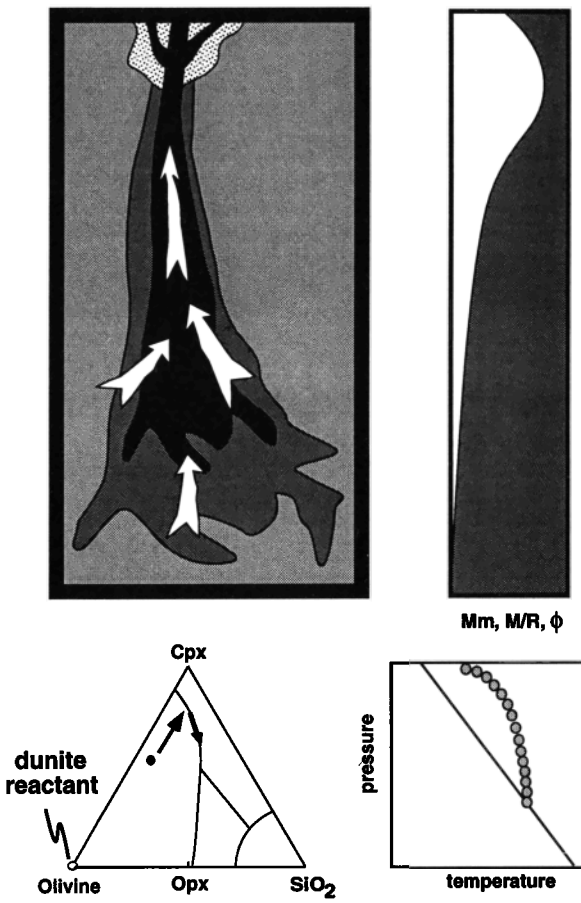

Figure 13. Structure of porous flow channels beneath a mid-ocean ridge and the geochemical consequences of this structure. Top left-hand diagram illustrates that porous flow will be mainly focused into discrete dissolution channels, composed of porous dunite. Top right shows that the melt fraction (Mm), melt/rock ratio (M/R), and porosity (ϕ) will all increase within porous flow channels almost to the base of the newly forming oceanic crust where liquid must cool and begin to crystallize. Phase diagram at bottom right illustrates the chemical effects of melt/rock reaction within the porous flow channel. The porous flow channel will be composed mainly of dunite, with which ascending magma will be saturated. There will be little or no compositional difference between magma transported through such a channel and magma which ascends in a chemically closed system.

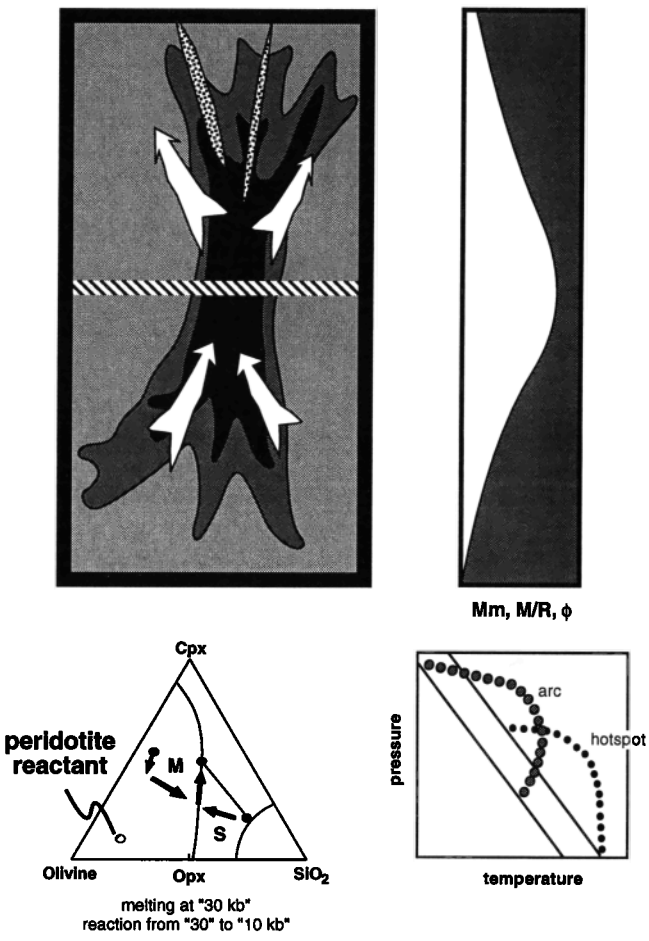

Figure 14. Structure of porous flow channels beneath an intraplate hot spot or a subduction-related magmatic arc. Ascending liquid in a closed system would initially be above its liquidus temperature, because liquid and solid ascend on a nearly adiabatic path in a mantle "plume" and because initial liquids in subduction zones must heat up as they rise beneath arcs. Higher, liquids pass into colder mantle and will themselves begin to cool and crystallize, leading to decreasing melt fraction (Mm), melt/rock ratio (M/R), and porosity (ϕ). In such conditions, melt migrating by porous flow may form flow conduits, with "walls" of low porosity. These conduits will gradually fill with products of magmatic crystallization and be abandoned, after which new flow conduits will form. Also shown are cracks formed as a result of magmatic overpressure in the tectosphere. The overall effect of such a flow structure is to produce increasingly small melt/rock ratios upsection, maximizing the chemical effects of melt/rock reaction on the composition of migrating liquids. Phase diagram at bottom right shows the chemical effects of slow cooling and rapid melt/rock reaction for an initial, picritic partial melt of the mantle reacting with mantle peridotite from 2 to 0.5 GPa (as in Figure 2c), labeled M, as well as for ascending partial melts of subducted crust, labeled S [e.g., *Carroll and Wyllie*, 1989; *Kelemen*, 1993; *Kelemen et al.*, 1993].

chemical effects of melt/rock reaction on the composition of migrating liquids. Specifically, melts will remain close to Fe/Mg equilibrium with mantle olivine and will retain high Ni and Cr concentrations, with increasing concentrations of magmaphile components, such as H_2O, CO_2, K, and incompatible trace elements [e.g., *Kelemen*, 1986; *Kelemen et al.*, 1992, 1993]. This is in accord with the idea that melt/rock reaction is important in producing magmas in subduction-related arcs [e.g., *Kay*, 1978; *Kelemen*, 1986, 1990, 1994; *Carroll and Wyllie*, 1989; *Kelemen et al.*, 1993] and above mantle hot spots [e.g., *Watson* 1993; *Wagner and Grove*, 1992]. The effects of melt/rock reaction may also be detected in samples of the continental tectosphere [e.g., *Menzies et al.*, 1985; *Navon and Stolper*, 1987; *Kelemen et al.*, 1992; *Rudnick et al.*, 1993] and in the oceanic tectosphere where it has been modified by hotspots [e.g., *Hauri et al.*, 1993; *Sen et al.*, 1993; *Salters and Zindler*, 1994].

Acknowledgments. We thank Robert Frazel for assistance in constructing the experimental apparatus; Greg Hirth, Art Thompson, Dan Rothman, Henry Dick, Stan Hart, Nobu Shimizu, Dan McKenzie, Mark Spiegelman, Adolphe Nicolas, Jean-Louis Bodinier, and Karl Helfrich for stimulating discussions; Mark Ghiorso for making the new version of his silicate liquid solution model available to us; and Bruce Marsh, Tony

Morse, and Claude Jaupart for encouraging us to present this paper. We also thank Alexander McBirney for bringing Chadam and Ortoleva's work to our attention many years ago. Interdisciplinary discussions in the Keck Geodynamics Seminar at Woods Hole initiated this project. Norm Sleep, Dave Scott and Anne Devaille provided careful reviews which substantially improved the manuscript. Early work was supported by the Woods Hole/MIT Joint Graduate Program in Oceanography (Aharonov, Jordahl), NSF grant EAR 9218819 and the sponsors of the MIT Porous Flow Project (Aharonov), NSF grants EAR 9005306, OCE 9217556, a Mellon Independent Study Award from the Woods Hole Oceanographic Institution (Kelemen), and EAR 8916857 (Whitehead). More recently, Aharonov, Kelemen, and Whitehead have been supported in this research by OCE 9314013.

References

Aharonov, E., J.A. Whitehead, and P.B. Kelemen, Channeling instability of melt flowing through the reactive, decompressing mantle, paper presented at the 20th International Conference on Mathematical Geophysics, National Science Foundation, Villefranche sur Mer, 1994.

Aho, A.E., Geology and genesis of ultrabasic nickel-copper-pyrrhotite deposits at the Pacific Nickel property, southwestern British Columbia, *Econ. Geol., 51*, 444-481, 1956.

Bédard, J.H., R.C. Kerr, and M.A. Hallworth, Porous sidewall and sloping floor crystallization experiments using a reactive mush: Implications for the self-channelization of residual melts in cumulates, *Earth Planet. Sci. Lett., 111*, 319-329, 1992.

Boudier, F., and A. Nicolas, Structural controls on partial melting in the Lanzo peridotites, in Magma Genesis, edited by H.J.B. Dick, *Oreg. Dep. Geol. Miner. Ind. Bull., 96*, 63-78, 1977.

Brearley, M., and C.M. Scarfe, Dissolution rates of upper mantle minerals in an alkali basalt melt at high pressure: An experimental study and implications for ultramafic xenolith survival, *J. Petrol., 27*, 1157-1182, 1986.

Butcher, A.R., I.M. Young, and J.W. Faithful, Finger structures in the Rhum complex, *Geol. Mag., 122*, 491-502, 1985.

Carlson, R.W., A matter of give and take, *Nature, 359*, 16-17, 1992.

Carroll, M.R., and P.J. Wyllie, Experimental phase relations in the system tonalite-peridotite-H2O: Implications for assimilation and differentiation processes near the crust-mantle boundary, *J. Petrol., 30*, 1351-1382, 1989.

Chadam, J., D. Hoff, P. Ortoleva, and A. Sen, Reactive-infiltration instability, *J. Appl. Math., 36*, 207-238, 1986.

Daccord, G., Chemical dissolution of a porous medium by a reactive fluid, *Phys. Rev. Lett., 58*, 479-482, 1987.

Daines, M.J., and F.M. Richter, An experimental method for directly determining the interconnectivity of melt in a partially molten system, *Geophys. Res. Lett. , 15*, 1459-1462, 1988.

Daines, M.J., and D.L. Kohlstedt, The transition from porous to channelized flow due to melt/rock reaction during melt migration, *Geophys. Res. Lett., 21*, 145-148, 1993.

Davies, J.H., and D.J. Stevenson, Physical model of source region of subduction zone volcanics, *J. Geophys. Res., 97*, 2037-2070, 1992.

d'Humiers, D., P. Lallemand, J.P. Boon, D. dab, and A. Noullez, Fluid dynamics with lattice gases, in *Chaos and Complexity*, edited by R. Livi, S. Ruffo, S. Cilberto, and M. Buiatti, pp. 278-301, World Scientific Publishers, Singapore, 1988.

Dick, H.J.B., Evidence of partial melting in the Josephine peridotite, in Magma Genesis, edited by H.J.B. Dick, *Oreg. Dept Geol. Miner. Ind. Bull., 96*, 63-78, 1977.

Dick, H. J. B., Abyssal peridotites, very slow spreading ridges and ocean ridge magmatism, in *Magmatism in the Ocean Basins*, edited by A. D. Saunders, and M. J. Norry, *Geol. Soc. Spec. Pub., 42*, 71-105, 1989.

Dick, H. J. B., R. L. Fisher, and W. B. Bryan, Mineralogic variability of the uppermost mantle along mid-ocean ridges, *Earth Planet. Sci. Lett., 69*, 88-106, 1984.

Faul, U.H., A.D. Johnston, and H.S. Waff, Melt distribution in partially molten lherzolite, *Eos Trans. AGU, 74*(43), Fall Meeting suppl., 660, 1993.

Flekkoy, E., Lattice BGK models for miscible fluids, *Phys. Rev. E, 47*, 4247-4257, 1993.

Frisch, U., B. Hasslacher, and Y. Pomeau, Lattice gas automata for the Navier-Stokes equation, *Phys. Rev. Lett., 56*, 1505-1508, 1986.

Garrido, C.J., M. Remaidi, J.-L. Bodinier, F. Gervilla, J. Torres-Ruiz, and P. Fenoll, Replacive pyroxenites in the Ronda orogenic lherzolite: Evidence for km-scale percolation of calc-alkaline melts in the upper mantle, *Terra Abstr., 1*, 147, 1993.

Ghiorso, M. S., Chemical mass transfer in magmatic processes, I, Thermodynamic relations and numerical algorithms, *Contrib. Mineral. Petrol., 90*, 107-120, 1985.

Ghiorso, M.S., and P.B. Kelemen, Evaluating reaction stoichiometry in magmatic systems evolving under generalized thermodynamic constraints: Examples comparing isothermal and isenthalpic assimilation, in: Magmatic Processes: Physicochemical Principles, edited by B.O. Mysen, *Spec. Pub. Geochem. Soc., 1*, (Yoder Volume), 319-336, 1987.

Ghiorso, M.S., and R.O. Sack, MELTS: Software for the thermodynamic analysis of phase equilibria in magmatic systems, *Geol. Soc. Am. Abstr. Programs, 25*, A-96, 1993.

Ghiorso, M.S., and R.O. Sack, Chemical mass transfer in magmatic processes, IV, *Contrib. Mineral. Petrol.*, in press, 1994.

Ghiorso, M. S., I. S. E. Carmichael, M. L. Rivers, and R. O. Sack, The Gibbs Free Energy of mixing of natural silicate liquids: An expanded regular solution approximation for the calculation of magmatic intensive variables, *Contrib. Mineral. Petrol., 85*, 107-145, 1983.

Hart, S.R., Equilibration during mantle melting: A fractal tree model, *Proc. Natl. Acad. Sci. U.S.A., 90*, 11,914-11,918, 1993.

Hauri, E.H., N. Shimizu, J.J. Dieu, and S.R. Hart, Evidence for hotspot-related carbonatite metasomatism in the oceanic upper mantle, *Nature, 365*, 221-227, 1993.

Henon, M., Viscosity of lattice gases, *Complex Syst., 1*, 763-789, 1987.

Hinch, E. J., and B. S. Bhatt, Stability of an acid front moving through porous rock, *J. Fluid. Mech., 212*, 279-288, 1990.

Hirose, K., and I. Kushiro, Partial melting of dry peridotites at high pressures: Determination of compositions of melts segregated from peridotite using aggregates of diamond, *Earth Planet. Sci. Lett., 114*, 477-489, 1993.

Hoefner, M.L., and H.S. Fogler, Pore evolution and channel formation during flow and reaction in porous media, *Am. Inst. Chem. Eng. J., 34*, 45-54, 1988.

Irvine, T.N., Petrology of the Duke Island ultramafic complex, southeastern Alaska, *Geol. Soc. Am., Mem. 138*, 240 pp., 1974.

James, O.B., Origin and emplacement of the ultramafic rocks of the Emigrant Gap area, *J. Petrol., 12*, 523-560, 1971.

Johnson, K.T.M., H.J.B. Dick, and N. Shimizu, Melting in the oceanic upper mantle: An ion microprobe study of diopsides in abyssal peridotites, J. *Geophys. Res., 95*, 2661-2678, 1990.

Johnson, K.T.M., and H.J.B. Dick, Open system melting and the temporal and spatial variation of peridotite and basalt compositions at the Atlantis II Fracture Zone, *J. Geophys. Res., 97*, 9219-9241, 1992.

Jordan, T. H., Structure and formation of the continental tectosphere, *J. Petrol., Special Lithosphere Issue*, 11-37, 1988.

Kay, R.W., Aleutian magnesian andesites: Melts from subducted Pacific ocean crust, *J. Volcanol. Geotherm. Res., 4*, 17-32, 1978.

Kelemen, P.B., Assimilation of ultramafic rock in subduction-related magmatic arcs, *J. Geol., 94*, 829-843, 1986.

Kelemen, P.B., Reaction between ultramafic wall rock and fractionating basaltic magma, I, Phase relations, the origin of calc-alkaline magma series, and the formation of discordant dunite, *J. Petrol., 31*, 51-98, 1990.

Kelemen, P.B., Genesis of high Mg# andesites and the continental crust, *Contrib. Mineral. Petrol.*, in press, 1994.

Kelemen, P.B., and H.J.B. Dick, Focused melt flow and localized deformation in the upper mantle: Juxtaposition of replacive dunite and ductile shear zones in the Josephine peridotite, SW Oregon. *J. Geophys. Res.*, in press, 1994.

Kelemen, P.B., and M.S. Ghiorso, Assimilation of peridotite in zoned calc-alkaline plutonic complexes: Evidence from the Big Jim complex,

Washington Cascades, *Contrib. Mineral. Petrol.*, *94*, 12-28, 1986.

Kelemen, P.B., H.J.B. Dick, and J.E. Quick, Production of harzburgite by pervasive melt-rock reaction in the upper mantle, *Nature* , *358*, 635-641, 1992.

Kelemen, P.B., N. Shimizu, and J.T. Dunn, Relative depletion of niobium in some arc magmas and the continental crust: Partitioning of K, Nb, La and Ce during melt/rock reaction in the upper mantle, *Earth Planet. Sci. Lett.*, *120*, 111-133, 1993.

Kinzler, R. J., and T. L. Grove, Primary magmas of mid-ocean ridge basalts 2. Applications, *J. Geophys. Res.*, *97*, 6907-6926, 1992.

Kuo, L.-C., and R. J. Kirkpatrick, Kinetics of crystal dissolution in the system diopside-forsterite-silica, *Am. J. Sci.*, *285*, 51-90, 1985.

Langmuir, C.H., E.M. Klein, and T. Plank, Petrological systematics of mid-ocean ridge basalts: Constraints on melt generation beneath mid-ocean ridges, in Mantle Flow and Melt Generation at Mid-Ocean Ridges, edited by J. Phipps Morgan, D.K. Blackman, and J.M. Sinton, *Geophys. Monogr. Ser.*, *vol. 71*, 183-280, 1992.

Leblanc, M., and G. Ceuleneer, Chromite crystallization in a multicellular magma flow: Evidence from a chromitite dike in the Oman ophiolite, *Lithos*, *27*, 231-257, 1992.

Lippard, S.J., A.W. Shelton, and I.G. Gass, *The Ophiolite of Northern Oman*, 178 pp., Blackwell Scientific, Oxford UK, 1986.

Maaloe, S., and A. Scheie, The permeability controlled accumulation of primary magma, *Contrib. Mineral. Petrol.*, *81*, 350-357, 1982.

McKenzie, D., The generation and compaction of partially molten rock, *J. Petrol. 25*, 713-765, 1984.

McKenzie, D., and M.J. Bickle, The volume and composition of melt generated by extension of the lithosphere, *J. Petrol.*, *29*, 625-679, 1988.

Menzies, M., P. Kempton, and M. Dungan, Interaction of continental lithosphere and aesthenospheric melts below the Geronimo Volcanic Field, Arizona, U.S.A, *J. Petrol.*, *26*, 663-693, 1985.

Navon, O., and E. Stolper, Geochemical consequences of melt percolation: The upper mantle as a chromatographic column, *J. Geol.*, *95*, 285-307, 1987.

Nicolas, A., *Structures of Ophiolites and Dynamics of Oceanic Lithosphere*, 367 pp., Kluwer Academic, Norwell, Mass., 1989.

Nicolas, A., Melt extraction from mantle peridotites: Hydrofracturing and porous flow, with consequences for oceanic ridge activity, in *Magma Transport and Storage*, edited by M.P. Ryan, pp. 159-174, J. Wiley & Sons, 1990.

Nixon, P., *Mantle Xenoliths*, 844 pp., John Wiley, New York, 1987.

Ortoleva P., J. Chadam, E. Merino, and A. Sen, Geochemical self-organization, II, The reactive-infiltration instability, *Am. J. Sci.*, *287*, 1008-1040, 1987.

Peacock, S.M., Numerical simulation of subduction zone pressure-temperature-time paths: Constraints on fluid production and arc magmatism, *Philos. Trans. R. Soc. London A*, *335*, 341-353, 1991.

Phillips, O. M., *Flow and Reactions in Permeable Rocks*, 285 pp., Cambridge University Press, New York, 1991.

Pokhilenko, N.P., N.V. Sobolev, and Y.G. Larent'ev, Xenoliths of diamondiferous ultramafic rocks from Yakutian kimberlites, paper presented at the Second International Kimberlite Conference, American Geophysical Union, Santa Fe, N. M., 1977.

Qian, Y.H., D d'Humieres, and P. Lallemand. Lattice BGK models for the Navier-Stokes equation. *Europhys. Lett.*, *17*(6), 479-484, 1992.

Quick, J.E., The origin and significance of large, tabular dunite bodies in the Trinity Peridotite, northern California, *Contrib. Mineral. Petrol.*, *78*, 413-422, 1981.

Rabinowicz, M., A. Nicolas, and J.-L. Vigneresse, A rolling mill effect in aesthenospheric flow beneath oceanic spreading centers, *Earth Planet. Sci. Lett.*, *67*, 97-108, 1984.

Rabinowicz, M., G. Ceuleneer, and A. Nicolas, Melt segregation and flow in mantle diapirs below spreading centers: Evidence from the Oman ophiolites, *J. Geophys. Res.*, *92*, 3475-3486, 1987.

Raedeke, L.D., and I..S. McCallum, Investigation in the Stillwater Complex, II, Petrology and petrogenesis of the ultramafic series, *J. Petrol.*, *25*, 395-420, 1984.

Remaidi, M., Étude petrologique et géochemique d'une association peridotites refractaires - pyroxenites dans le massif de Ronda (Espagne), Ph.D. thesis, Univ. de Montpellier, France, 1993.

Riley, G.N., Jr., and D.L. Kohlstedt, Kinetics of melt migration in upper mantle type rocks, *Earth Planet. Sci. Lett.*, *105*, 500-521, 1991.

Rothman, D.H., Cellular-automaton fluids: A model for flow in porous media, *Geophysics*, *53*, 509-518, 1988.

Rudnick, R. L., W. F. McDonough, and B. W. Chappell, Carbonatite metasomatism in the northern Tanzanian mantle: Petrographic and geochemical characteristics, *Earth Planet. Sci. Lett.*, *114*, 463-475, 1993.

Salters, V.J.M., and S.R. Hart, The Hf-paradox and the role of garnet in the MORB source, *Nature*, *342*, 420-422, 1989.

Salters, V.J.M., and A. Zindler, Extreme $^{176}Hf/^{177}Hf$ in the sub-oceanic mantle and the origin of high field strength element depletions in the mantle, *Earth Planet. Sci. Lett.*, in press, 1994.

Savel'yeva, G.N., S.A. Shcherbakov, and Y.A. Denisova, The role of high-temperature deformation in the development of dunite bodies in harzburgites, *Geotectonics*, *14*, 175-182, 1980.

Scott, D.R., and D.J. Stevenson, A self-consistent model of melting, magma migration and buoyancy driven circulation beneath mid-ocean ridges, *J. Geophys. Res.*, *94*, 2973-2988, 1989.

Sen, G., and R. E. Jones, Cumulate xenolith in Oahu, Hawaii: Implications for deep magma chambers and Hawaiian volcanism, *Science*, *249*, 1154-1157, 1990.

Sen, G., F. A. Frey, N. Shimizu, and W. P. Leeman, Evolution of the lithosphere beneath Oahu, Hawaii: Rare earth element abundances in mantle xenoliths, *Earth Planet. Sci. Lett.*, *119*, 53-69, 1993.

Sleep, N.H., Formation of oceanic crust: Some thermal constraints, *J. Geophys. Res.*, *80*, 4037-4042, 1975.

Sleep, N.H., Tapping of melt by veins and dykes, *J. Geophys. Res.*, *93*, 10,255-10,272, 1988.

Sobolev, N.V., Y. G. Lavrent'yev, N.P. Pokhilenko, and L.V. Usova, Chrome-rich garnets from the kimberlites of Yakutia and their paragenesis, *Contrib. Mineral. Petrol.*, *40*, 39-52, 1973.

Spiegelman, M., Physics of melt extraction: Theory, implications and applications, *Philos. Trans. R. Soc. London A*, *342*, 23-41, 1993.

Speigelman, M., and D. McKenzie, Simple 2-D models for melt extraction at mid-ocean ridges and island arcs, *Earth Planet. Sci. Lett.*, *83*, 137-152, 1987.

Speigelman, M., and P. Kenyon, The requirements for chemical disequilibrium during melt migration, *Earth Planet. Sci. Lett.*, *109*, 611-620, 1992.

Steefel, C., and A. Lasaga, Evolution of dissolution patterns: Permeability change due to coupled flow and reactions, in *Chemical Modeling in Aqueous Systems II*, edited by D.C. Melchior, and R.L. Bassett, *Symp. Ser. 416*, pp. 212-225, American Chemical Society, Washington, D.C., 1990.

Stevenson, D., Spontaneous small-scale melt segregation in partial melts undergoing deformation, *Geophys. Res. Lett.*, *9*, 1067-1070, 1989.

Stolper, E., A phase diagram for mid-ocean ridge basalts: Preliminary results and implications for petrogenesis, *Contrib. Mineral. Petrol.*, *74*, 13-27, 1980.

Stumpfl, E.F., and J.C. Rucklidge, The platiniferous dunite pipes of the eastern Bushveld, *Econ. Geol.*, *77*, 1419-1431, 1982.

Tait, S., and C. Jaupart, Compositional convection in a reactive crystalline mush and melt differentiation, *J. Geophys. Res.*, *97*, 6735-6756, 1991.

Tait, S., K. Jahrling, and C. Jaupart, The planform of compositional convection in a mushy layer, *Nature*, *359*, 406-408, 1992.

Takahashi, N., Evidence for melt segregation towards fractures in the Horoman mantle peridotite complex, *Nature*, *359*, 52-55, 1992.

Toramaru, A., and N. Fujii, Connectivity of melt phase in a partially molten peridotite, *J. Geophys. Res.*, *91*, 9239-9252, 1986.

Von Bargen, N., and H.S. Waff, Wetting of enstatite by basaltic melt at 1350°C and 1-25 GPa pressure, *J. Geophys. Res.*, *93*, 1153-1158, 1988.

Waff, H.S., and U.H. Faul, Effects of crystalline anisotropy on fluid distribution in ultramafic partial melts, *J. Geophys. Res.*, *97*, 9003-9014, 1992.

Wagner, T.P., and T.L. Grove, Primary magmas of the Hawaiian plume: Experimental evidence bearing on the plume paradox, *Eos Trans. AGU, 73*(43), Fall Meeting suppl., 615, 1992.

Watson, E.B., Melt infiltration and magma evolution, *Geology, 10*, 236-240, 1982.

Watson, S., Rare earth element inversions and percolation models for Hawaii, *J. Petrol., 34*, 763-783, 1993.

Whitehead J.A., and K.R. Helfrich, Instability of flow with temperature-dependent viscosity: A model of magma dynamics, *J. Geophys. Res., 96*, 4145-4146, 1991.

Whitehead, J.A., and P.B. Kelemen, Thermal and chemical corrosion in partially molten mantle, in *Magmatic Systems*, edited by M. P. Ryan, pp. 355-379, Academic, San Diego, Calif., 1994.

Yoder, H.S., *Generation of Basaltic Magmas*, 264 pp., National Academy of Sciences, Washington DC, 1976.

Zhang, Y., D. Walker, and C.E. Lesher, Diffusive crystal dissolution, *Contrib. Mineral. Petrol., 102*, 492-513, 1989.

E. Aharonov, WHOI/MIT Joint Graduate Program in Oceanography, Department of Earth, Atmospheric, and Planetary Sciences, Massachusetts Institute of Technology, Cambridge, MA 02139. (email: einat@segovia.mit.edu).

K. A. Jordahl, WHOI/MIT Joint Graduate Program in Oceanography, Woods Hole Oceanographic Institution, Woods Hole, MA 02543.

P. B. Kelemen, Department of Geology and Geophysics, Woods Hole Oceanographic Institution, Woods Hole, MA 02543. (email: peterk@cliff.whoi.edu).

J. A. Whitehead, Department of Physical Oceanography, Woods Hole Oceanographic Institution, Woods Hole, MA 02543. (email: jwhitehead@whoi.edu).

(Received February 15, 1994; revised August 19, 1994; accepted September 22, 1994.)